# Relativistic description of nuclear systems in the Hartree-Fock approximation

A. Bouyssy, J.-F. Mathiot, and Nguyen Van Giai
*Division de Physique Théorique, Institut de Physique Nucléaire, F-91406, Orsay Cédex, France*

S. Marcos
*Department of Physics, University of Santander, Santander, Spain*
(Received 3 April 1986; revised manuscript received 29 January 1987)

The structure of infinite nuclear matter and finite nuclei is studied in the framework of the relativistic Hartree-Fock approximation. Particular attention is paid to the contribution of isovector mesons ($\pi$,$\rho$). A satisfactory description of binding energies and densities can be obtained for light as well as heavy nuclei. The spin-orbit splittings are well reproduced. Connections with nonrelativistic formulations are also discussed.

## I. INTRODUCTION

It is now generally recognized that the nucleon-nucleon interaction is mediated by the exchange of mesons, isoscalar as well as isovector, and this has been repeatedly tested, directly or indirectly, in the past. The understanding of nuclear structure at the microscopic level, therefore, has to be achieved in the same language, i.e., with the same degrees of freedom. From a nonrelativistic point of view, which is the one that has received most attention, this program leads to the study of infinite nuclear matter from different approaches, one being the Bethe-Brueckner theory of many body systems.[1] The microscopic description of finite nuclei, however, is far from being so complete, in the sense that effective interactions depending on the baryonic density have to be constructed in order to account for ground state properties. These interactions are either semiphenomenological and incorporate what is known about the $G$ matrix in infinite matter, or entirely phenomenological. A typical example is the well known Skyrme interaction[2] and its various modifications. This program has reached a very high degree of accuracy and is essential in the development of nuclear structure studies in the last decade.

On the other hand, the description of nucleon and meson degrees of freedom has to rely ultimately on a relativistic quantum field formulation in order to include the full structure of nuclear medium (to describe, for instance, its spin structure). In this scheme new mechanisms arise naturally and are associated with negative energy solutions of the Dirac equation for the fermion field. Such mechanisms are already well known in intermediate energy physics and give rise to large meson exchange current contributions for isovector electromagnetic transitions, for instance. It is then interesting to examine whether these mechanisms play an important role in nuclear structure at normal density. For a qualitative estimate of these relativistic effects, together with genuine kinematical corrections, we remark that the mean value of the nucleon velocity in the medium is not at all negligible and can be as large as 0.4 times the velocity of light.

This ambitious program has been initiated more than ten years ago in the context of the mean field approximation.[3,4] The structure of the vacuum (polarization of the Dirac sea) has then been studied[5] in that framework. Subsequent developments were restricted to the tree approximation (vacuum fluctuations are not taken into account) and concern the structure of finite nuclei in the same mean field approximation, i.e., the Hartree approximation,[6–9] or the description of nuclear matter in either the Hartree-Fock[10,11] (HF) or Brueckner-Hartree-Fock[12,13] (BHF) approximation. Derivation of the HF equations in finite nuclei has been performed but restricted to the study of hypernuclei.[14] In addition to the linear coupling of the meson fields to the nucleon field (which gives rise to the NN potential in free space), one can also incorporate, in that formulation of nuclear structure, nonlinear couplings of meson fields and, in particular, of the scalar field [according to a chiral symmetric extension of the ($\sigma$,$\omega$) model]. This has been studied in nuclear matter[15,16] and further extended to finite nuclei.[16] Such studies depend on the strength of these new couplings and these have to be treated as new parameters in order to get reasonable results. All these developments are discussed in detail in a recent review article.[17] In the case of atomic physics, the relativistic HF problem has been extensively studied by several authors (see, for instance, Ref. 18).

In this work we present a consistent description of infinite nuclear matter and finite nuclei in the framework of the Hartree-*Fock* approximation to the complete relativistic quantum field approach. In this scheme the isovector mesons can play an important role, and in particular, the lightest ones (pion and rho mesons), as has already been found in the context of nonrelativistic formulations. Of course, for these mesons the dominant contributions come from exchange terms and one cannot limit oneself just to the Hartree approximation. We shall investigate these exchange corrections, which must be part of any more complete theory. We discuss throughout this paper the peculiarity of the relativistic approach and try to make some connection with standard HF calculations, especially those based on the Skyrme effective interaction. We detail in Sec. II the basic features of the model Hamiltonian. The structure of infinite nuclear matter is studied in Sec.

 

III and the ground state properties of closed shell nuclei are discussed in Sec. IV. General conclusions are drawn in the last section.

## II. THE NUCLEAR HAMILTONIAN

### A. The model Lagrangian

According to the one boson exchange (OBE) description of the NN interaction, we start from an effective Lagrangian density constructed from the degrees of freedom associated with two isoscalar mesons ($\sigma$ and $\omega$) and two isovector ones ($\pi$ and $\rho$) with the following quantum numbers ($J^\pi, T$):

$$\sigma(0^+,0),\ \omega(1^-,0),\ \pi(0^-,1),\ \rho(1^-,1)\ .$$

The $\sigma$ meson is introduced to simulate, in the HF approximation, the correlated two-pion exchange potential in a relative $S$ state. The Lagrangian density is written as

$$\mathscr{L}=\mathscr{L}_0+\mathscr{L}_I\ . \tag{1}$$

The free Lagrangian density $\mathscr{L}_0$ is given by

$$\begin{aligned}\mathscr{L}_0=&\bar{\psi}(i\gamma_\mu\partial^\mu-M)\psi+\tfrac{1}{2}(\partial_\mu\sigma\partial^\mu\sigma-m_\sigma^2\sigma^2)\\&+\tfrac{1}{2}m_\omega^2\omega_\mu\omega^\mu-\tfrac{1}{4}F_{\mu\nu}F^{\mu\nu}+\tfrac{1}{2}m_\rho^2\boldsymbol{\rho}_\mu\cdot\boldsymbol{\rho}^\mu\\&-\tfrac{1}{4}\mathbf{G}_{\mu\nu}\cdot\mathbf{G}^{\mu\nu}+\tfrac{1}{2}(\partial_\mu\boldsymbol{\pi}\cdot\partial^\mu\boldsymbol{\pi}-m_\pi^2\boldsymbol{\pi}^2)-\tfrac{1}{4}H_{\mu\nu}H^{\mu\nu}\ ,\end{aligned} \tag{2}$$

with

$$\begin{aligned}F_{\mu\nu}&=\partial_\nu\omega_\mu-\partial_\mu\omega_\nu\ ,\\ \mathbf{G}_{\mu\nu}&=\partial_\nu\boldsymbol{\rho}_\mu-\partial_\mu\boldsymbol{\rho}_\nu\ ,\\ H_{\mu\nu}&=\partial_\nu A_\mu-\partial_\mu A_\nu\ .\end{aligned} \tag{3}$$

Here, $M$, $m_\sigma$, $m_\omega$, $m_\pi$, and $m_\rho$ are the rest masses of the nucleon and mesons. The field operators are denoted by $\psi$ for the nucleon and by $\sigma$, $\omega_\mu$, $\boldsymbol{\pi}$, and $\boldsymbol{\rho}_\mu$ for the meson fields, while $A_\mu$ is the electromagnetic field. All fields are function of $x=(\mathbf{x},t)$. The Bjorken-Drell conventions[19] are used throughout this paper. Note that $\boldsymbol{\rho}_\mu$ and $\boldsymbol{\pi}$ are vectors in isospin space. The interaction Lagrangian density is given by

$$\begin{aligned}\mathscr{L}_I=&-g_\sigma\bar{\psi}\sigma\psi-g_\omega\bar{\psi}\gamma_\mu\omega^\mu\psi+\frac{f_\omega}{2M}\bar{\psi}\sigma_{\mu\nu}\partial^\nu\omega^\mu\psi\\&-g_\rho\bar{\psi}\gamma_\mu\boldsymbol{\rho}^\mu\cdot\boldsymbol{\tau}\psi+\frac{f_\rho}{2M}\bar{\psi}\sigma_{\mu\nu}\partial^\nu\boldsymbol{\rho}^\mu\cdot\boldsymbol{\tau}\psi\\&-e\bar{\psi}\gamma_\mu\tfrac{1}{2}(1+\tau_3)A^\mu\psi+\mathscr{L}_{\pi\mathrm{NN}}\ ,\end{aligned} \tag{4}$$

where $\boldsymbol{\tau}$ and $\tau_3$ are the usual isospin Pauli matrices. The quantities $g_i$ ($i=\sigma,\omega,\pi,\rho$) are the effective meson-nucleon coupling constants, while $f_\omega$ and $f_\rho$ are the isoscalar- and isovector-tensor coupling constants, and $e^2=4\pi\alpha$.

The $\pi$NN interaction Lagrangian $\mathscr{L}_{\pi\mathrm{NN}}$ can be written into two possible forms. One can use either the pseudoscalar (ps) coupling,

$$\mathscr{L}^{\mathrm{ps}}_{\pi\mathrm{NN}}=-ig_\pi\bar{\psi}\gamma_5\boldsymbol{\pi}\cdot\boldsymbol{\tau}\psi\ , \tag{5}$$

or the pseudovector (pv) one,

$$\mathscr{L}^{\mathrm{pv}}_{\pi\mathrm{NN}}=-\frac{f_\pi}{m_\pi}\bar{\psi}\gamma_5\gamma_\mu\partial^\mu\boldsymbol{\pi}\cdot\boldsymbol{\tau}\psi\ . \tag{6}$$

Both couplings lead to the one-pion exchange potential in the nonrelativistic limit for on-shell nucleons if their corresponding coupling constants satisfy the equivalence relation

$$\frac{g_\pi}{2M}=\frac{f_\pi}{m_\pi}\ . \tag{7}$$

In the HF approximation, however, one has to use the form which incorporates, at that order, the dominant physical process. It is well known from general arguments (chiral symmetry) and from the construction of the NN potential (with pair suppression mechanism) that the pseudovector coupling has to be used to get reasonable results in the one-pion exchange approximation. We then choose the pv coupling in this work.

The construction of the effective Lagrangian is dictated by low-energy phenomenology, and, in particular, by the construction of the NN potential. In this spirit, tensor couplings for vector mesons have to be taken into account, in principle. For the $\omega$ meson, the tensor coupling is small and will not be considered in the numerical part of this work. Furthermore, the presence of tensor couplings implies that the model Lagrangian is no longer renormalizable and all physical observables should be calculated at the tree level. We shall adopt this point of view in the following developments.

### B. Equations of motion

In order to construct the Hamilton operator in nucleon space, starting with the effective Lagrangian (1), we require that the action be stationary for variations of any physical field $\phi$:

$$\delta\int_{t_1}^{t_2}dt\int d^3x\,\mathscr{L}(\mathbf{x},t)=0\ . \tag{8}$$

This leads to the canonical field equations:

$$\frac{\partial\mathscr{L}}{\partial\phi}-\partial^\mu\frac{\partial\mathscr{L}}{\partial[\partial^\mu\phi]}=0\ . \tag{9}$$

The corresponding Euler-Lagrange equations for the meson field operators can then be obtained. For instance, the $\sigma$ and $\omega$ fields are solutions of

$$\begin{aligned}&(\Box+m_\sigma^2)\sigma=-g_\sigma\bar{\psi}\psi\ ,\\&\partial^\mu F_{\nu\mu}+m_\omega^2\omega_\nu=g_\omega\bar{\psi}\gamma_\nu\psi\ .\end{aligned} \tag{10}$$

The first equation is an inhomogeneous Klein-Gordon equation, while the second one is a Proca equation with source terms. However, if the nucleon current satisfies the continuity equation

$$\partial^\mu[\bar{\psi}\gamma_\mu\psi]=0\ , \tag{11}$$

the Proca equation reduces to a Klein-Gordon equation:

$$(\Box+m_\omega^2)\omega_\nu=g_\omega\bar{\psi}\gamma_\nu\psi\ . \tag{12}$$

Solving the equation for the $\sigma$ meson field, one then obtains

$$\sigma(x)=-g_\sigma\int d^4y\, D_\sigma(x-y)\bar{\psi}(y)\psi(y)\ , \tag{13}$$

where $D_\sigma(x-y)$ is the retarded Green function of the Klein-Gordon equation. Similar expressions are deduced for the other mesons. On the other hand, if the Euler-Lagrange equation is written for the baryon field $\psi$, one gets a Dirac equation with source terms. This equation cannot, however, be solved exactly and one has to treat it in an appropriate approximation scheme, namely the HF approximation.

### C. An approximate Hamiltonian for Hartree-Fock calculations

The Hamilton operator is formally obtained through the general Legendre transformation

$$H(t)=\int d^3x\left[\sum_{\substack{i=\sigma,\omega,\\ \pi,\rho,\mathrm{N}}}\pi_i(\mathbf{x},t)\frac{\partial\phi_i(\mathbf{x},t)}{\partial t}-\mathscr{L}(\mathbf{x},t)\right], \tag{14}$$

where

$$\pi_i(\mathbf{x},t)=\frac{\partial\mathscr{L}}{\partial[\partial\phi_i/\partial t]}$$

is the conjugate momentum of the field operator $\phi_i(\mathbf{x},t)$. This leads to the general exact form for the Hamiltonian in nucleon space:

$$H=\int_{t=0}\bar{\psi}(x)(-i\boldsymbol{\gamma}\cdot\boldsymbol{\nabla}+M)\psi(x)d^3x +\tfrac{1}{2}\sum_{\substack{i=\sigma,\omega,\\ \rho,\pi}}\int_{t=0}\bar{\psi}(x)\bar{\psi}(x')\Gamma_i(1,2)\psi(x')\psi(x)d^3x\,d^4x'\ , \tag{15}$$

where the $\Gamma_i$ will be discussed later.

In order to obtain the Hartree-Fock equations, one possibility is to use the Dyson equation for the baryon propagator.[11] It is possible to arrive at the same result by defining an approximate effective Hamiltonian in the following way. We look for approximate field operators $\psi_0(x)$ satisfying a Dirac equation with a self-energy $\Sigma$ to be determined self-consistently:

$$(-i\gamma^\mu\partial_\mu+M+\Sigma)\psi_0(x)=0\ . \tag{16}$$

By replacing the exact $\psi(x)$ in Eq. (15) by the approximate $\psi_0(x)$, we obtain an effective Hamiltonian $H_0$. The expectation value of $H_0$ in the Hartree-Fock state (Slater determinant) gives an energy $E_0$. When we minimize $E_0$ with respect to $\Sigma$, we shall obtain equations for $\Sigma$ which will be seen to be identical to those obtained by the Dyson equation method.[11]

The two-body interactions mediated by the exchange of mesons are clearly not instantaneous. In this work, which deals with the HF description of nuclear ground states, we shall make the simplifying assumption of neglecting the time dependence of the meson fields, i.e., neglecting the time component of the four-momentum carried by the meson. This assumption has no consequence on the direct (Hartree) terms, while for the exchange (Fock) terms it amounts to neglecting retardation effects. The energy transfers involved are small compared to the masses of the exchanged mesons, so that this approximation should be valid for the $\sigma$-, $\omega$-, and $\rho$-induced interactions, and also, to a lesser extent, for the pion.

The approximate nucleon field operators $\psi_0(x)$ and $\psi_0^\dagger(x)$ are then expanded on the set of creation and annihilation operators defined by the stationary solutions of Eq. (16), still to be determined:

$$\begin{aligned}\psi_0(x)&=\sum_\alpha[f_\alpha(\mathbf{x})e^{-iE_\alpha t}b_\alpha+g_\alpha(\mathbf{x})e^{iE'_\alpha t}d_\alpha^\dagger]\ ,\\ \psi_0^\dagger(x)&=\sum_\alpha[f_\alpha^\dagger(\mathbf{x})e^{iE_\alpha t}b_\alpha^\dagger+g_\alpha^\dagger(\mathbf{x})e^{-iE'_\alpha t}d_\alpha]\ .\end{aligned} \tag{17}$$

Here, $f_\alpha(\mathbf{x})$ and $g_\alpha(\mathbf{x})$ are complete sets of Dirac spinors, $b_\alpha$ and $b_\alpha^\dagger$ represent annihilation and creation operators for nucleons in a state $\alpha$, while $d_\alpha$ and $d_\alpha^\dagger$ are the corresponding operators for antinucleons. In this work we study exchange corrections to the mean field approach and therefore we keep the same level of approximation, i.e., the $d$ and $d^\dagger$ terms are omitted in Eq. (17). Thus, the neglected terms will correspond to the self-consistent negative energy states.

The approximate Hamiltonian $H_0$ can now be expressed in second quantized form in terms of the fermion operators $b$ and $b^\dagger$. Following Eq. (15), it takes, in the momentum representation, the form

$$H_0=T+\sum_i V_i\ , \tag{18}$$

where

$$T=\sum_{\substack{p_1,p_2\\ \alpha_1,\alpha_2}}\bar{u}(p_1,\alpha_1)(\boldsymbol{\gamma}\cdot\mathbf{p}+M)u(p_2,\alpha_2)b^\dagger_{p_1\alpha_1}b_{p_2\alpha_2}\ , \tag{19}$$

$$V_i=\sum_{p_1,p_2q}\sum_{\substack{\alpha_1,\alpha_2\\ \alpha'_1,\alpha'_2}}(\text{isospin})\bar{u}(p_1+q,\alpha'_1)\bar{u}(p_2-q,\alpha'_2)\Gamma_i(1,2)\frac{1}{m_i^2+\mathbf{q}^2}u(p_2,\alpha_2)u(p_1,\alpha_1)b^\dagger_{p_1+q,\alpha'_1}b^\dagger_{p_2-q,\alpha'_2}b_{p_2,\alpha_2}b_{p_1,\alpha_1}\ . \tag{20}$$

In these equations, $u(\mathbf{p},\alpha)$ is a positive-energy spinor corresponding to a state with four-momentum $p=(p_0,\mathbf{p})$, and spin and isospin quantum numbers denoted by $\alpha$. The isospin factor is 1 for isoscalar mesons and $\tau_1\cdot\tau_2$ for isovector ones. The index $\alpha$ will be omitted in the following in order to shorten the notation. The various operators $\Gamma_i(1,2)$ are listed below:

$$\Gamma_\sigma(1,2)=-g_\sigma^2 ,$$
$$\Gamma_\omega(1,2)=g_\omega^2\gamma_\mu(1)\gamma^\mu(2) ,$$
$$\Gamma_\pi^{ps}(1,2)=g_\pi^2\gamma_5(1)\gamma_5(2) ,$$
$$\Gamma_\pi^{pv}(1,2)=-\left[\frac{f_\pi}{m_\pi}\right]^2(q\gamma_5)_1(q\gamma_5)_2 , \tag{21}$$
$$\Gamma_\rho^V(1,2)=g_\rho^2\gamma_\mu(1)\gamma^\mu(2) ,$$
$$\Gamma_\rho^T(1,2)=\left[\frac{f_\rho}{2M}\right]^2 q_\nu\sigma^{\mu\nu}(1)q^\lambda\sigma_{\mu\lambda}(2) ,$$
$$\Gamma_\rho^{VT}(1,2)=i\frac{f_\rho g_\rho}{2M}[\gamma_\mu(2)\sigma^{\mu\nu}(1)q_\nu-\sigma^{\mu\nu}(2)q_\nu\gamma_\mu(1)] .$$

### D. Nonrelativistic reductions

It is instructive to derive the nonrelativistic expansion of the vertex functions deduced from the interaction Lagrangian (4) for the different mesons. The nucleon spinor is taken to be the free Dirac spinor in the limit $p \ll M$:

$$u(\mathbf{p},s)\simeq\begin{bmatrix}1\\ \frac{\boldsymbol{\sigma}\cdot\mathbf{p}}{2M}\end{bmatrix}\chi_s , \tag{22}$$

where $\chi$ is the two-component spin wave function, and isospin indices have been omitted. For the $\sigma$ meson and the time component of the $\omega$ meson, for instance, we obtain

$$(2E_\omega)^{1/2}\langle {}^\omega_\sigma\mathrm{N}(p_f)\,|\,\mathscr{L}_I^{\overset{\omega}{\sigma}}\,|\,\mathrm{N}(p_i)\rangle = g_{\substack{\omega\\ \sigma}}\chi_f^\dagger\left[1-\frac{(\mathbf{p}_f\mp\mathbf{p}_i)^2}{8M^2}\pm i\boldsymbol{\sigma}\cdot\frac{\mathbf{p}_f\times\mathbf{p}_i}{4M^2}\right]\chi_i , \tag{23a}$$

whereas for the $\pi$ and $\rho$ mesons we have

$$\sqrt{2E_\pi}\langle\pi\mathrm{N}(p_f)\,|\,\mathscr{L}_I^\pi\,|\,\mathrm{N}(p_i)\rangle=ig_\pi\chi_f^\dagger\frac{\boldsymbol{\sigma}\cdot(\mathbf{p}_f-\mathbf{p}_i)}{2M}\chi_i , \tag{23b}$$

$$\sqrt{2E_\rho}\langle\rho\mathrm{N}(p_f)\,|\,\mathscr{L}_I^\rho\,|\,\mathrm{N}(p_i\rangle=ig_\rho\chi_f^\dagger\boldsymbol{\epsilon}\cdot\frac{\boldsymbol{\sigma}\times(\mathbf{p}_f-\mathbf{p}_i)}{2M}\chi_i , \tag{23c}$$

where $\boldsymbol{\epsilon}$ is the polarization of the $\rho$ meson.

The $\sigma$ and $\omega$ vertex functions are of zeroth order in a $1/M$ expansion and are consequently dominant. The third term in Eq. (23a) gives rise to the spin-orbit potential in finite nuclei. The NN potential associated with these mesons would be, to lowest order,

$$V_{\substack{\sigma\\ \omega}}(\mathbf{r}_1,\mathbf{r}_2)=\mp\frac{g_{\substack{\sigma\\ \omega}}^2}{4\pi}\frac{e^{-m_{\substack{\sigma\\ \omega}}|\mathbf{r}_1-\mathbf{r}_2|}}{|\mathbf{r}_1-\mathbf{r}_2|} , \tag{24}$$

and, according to the overall sign for the $\sigma$ and $\omega$ contributions, the spin-orbit contributions coming from these mesons add constructively. In infinite nuclear matter, these contributions to the NN potential will introduce scalar and timelike vector self-energies (represented schematically in Fig. 1). of the order of $-400$ and $+350$ MeV in the equation of motion for the nucleon, for typical values of the $\sigma$-N and $\omega$-N coupling constants. These large self-energies motivate the relativistic calculations of nuclear structure. The $\pi$ and $\rho$ vertex factors are of order $1/M$ and can be already considered as relativistic corrections. In the limit of small momentum transfers, the $\pi$- and $\rho$-exchange contributions are expected to be small. The momentum dependence of all these vertex factors is important in the sense that it will give additional contributions to the electromagnetic current (meson exchange currents) in order to keep the current conserved.

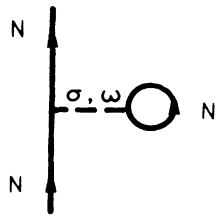


FIG. 1. Baryon self-energy in the Hartree approximation. The summation is restricted to the Fermi sea.

### E. Pion and rho exchange potentials

The NN potential deduced from the vertex factors (23b) and (23c) is usually decomposed into a central part and a tensor part. In the case of the $\pi$-exchange potential, for instance, one has

$$V_\pi(\mathbf{q})=\tfrac{-1}{3}\left[\frac{f_\pi}{m_\pi}\right]^2\frac{1}{m_\pi^2+\mathbf{q}^2}[(3\boldsymbol{\sigma}_1\cdot\mathbf{q}\,\boldsymbol{\sigma}_2\cdot\mathbf{q}-\boldsymbol{\sigma}_1\cdot\boldsymbol{\sigma}_2\mathbf{q}^2) +\boldsymbol{\sigma}_1\cdot\boldsymbol{\sigma}_2\mathbf{q}^2]\boldsymbol{\tau}_1\cdot\boldsymbol{\tau}_2$$
$$\equiv V_\pi^T(\mathbf{q})+V_\pi^c(\mathbf{q}) . \tag{25}$$

The tensor part (tensor of rank 2 in the momentum transfer) gives no contribution to the binding energy in the HF approximation. The central part can be rewritten as

$$V_\pi^c(\mathbf{q})=\tfrac{-1}{3}\left[\frac{f_\pi}{m_\pi}\right]^2\boldsymbol{\sigma}_1\cdot\boldsymbol{\sigma}_2\,\boldsymbol{\tau}_1\cdot\boldsymbol{\tau}_2\left[1-\frac{m_\pi^2}{m_\pi^2+\mathbf{q}^2}\right] . \tag{26}$$

If we Fourier-transform this expression, we get a repulsive contact interaction and an attractive Yukawa potential:

$$V_\pi^c(\mathbf{r})=\frac{-m_\pi^3}{12\pi}\left[\frac{f_\pi}{m_\pi}\right]^2\boldsymbol{\sigma}_1\cdot\boldsymbol{\sigma}_2\,\boldsymbol{\tau}_1\cdot\boldsymbol{\tau}_2\left[\frac{4\pi}{m_\pi^3}\delta(\mathbf{r})-\frac{e^{-m_\pi r}}{m_\pi r}\right] , \tag{27}$$

and a similar expression for the central potential coming from the $\rho$ exchange (with a strength 2 times larger). In a realistic many-body calculation, such $\delta(\mathbf{r})$ contributions would be suppressed by short-range correlations due to the repulsion of the NN potential at short distances ($\omega$ exchange). The resulting contribution (Yukawa term) is

consequently attractive.

By analogy with what is done in nonrelativistic calculations, and following the above procedure, one way to simulate the effect of short-range correlations on both $\pi$ and $\rho$ contributions is to remove such spurious $\delta$ components from the potential part of the nuclear Hamiltonian. This is done by subtracting the zero-rank tensor part of the NN potential coming from $\pi$ (pv coupling) and $\rho$ (tensor coupling) exchanges given by

$$\delta[\Gamma_{\pi,\rho}(1,2)]=\frac{1}{4\pi q^2}\int d\Omega_q \Gamma_{\pi,\rho}(1,2)\ , \tag{28}$$

where $\Gamma_\pi,\Gamma_\rho$ are given in Eq. (21).

It is expected that a more complete treatment of $\sigma$ and $\omega$ contributions which includes correlations will only modify the values of their coupling constants. To have the same self-energies in a correlated or uncorrelated calculation, one needs smaller coupling constants in the latter case. This is the basis for adjusting the isoscalar coupling constants in our approach.

## III. NUCLEAR MATTER

### A. Hartree-Fock equations

We consider now the baryon self-energy $\Sigma$ produced by the meson exchanges. Because of time-reversal and rotational invariance, it can be written quite generally as

$$\Sigma(\mathbf{p})=\Sigma_S(p)+\gamma_0\Sigma_0(p)+\boldsymbol{\gamma}\cdot\hat{\mathbf{p}}\Sigma_V(p)\ , \tag{29}$$

where $\hat{\mathbf{p}}$ is the unit vector along $\mathbf{p}$. Here, we have omitted the tensor piece $\gamma_0\boldsymbol{\gamma}\cdot\hat{\mathbf{p}}\Sigma_T(p)$, which does not appear in the HF approximation for nuclear matter. The different components of $\Sigma$, the scalar, time component and space component of the vector, are functions of $p=(E(p),\mathbf{p})$. The spinors in the infinite medium are solutions of the following Dirac equation:

$$[\boldsymbol{\gamma}\cdot\mathbf{p}^*+M^*]u(\mathbf{p},s)=\gamma_0 E^* u(\mathbf{p},s)\ , \tag{30}$$

where the starred quantities are defined by

$$\begin{aligned}\mathbf{p}^*(p)&=\mathbf{p}+\hat{\mathbf{p}}\Sigma_V(p)\ ,\\ M^*(p)&=M+\Sigma_S(p)\ ,\\ E^*(p)&=E(p)-\Sigma_0(p)\ .\end{aligned} \tag{31}$$

Here, $M^*$ is the usual scalar effective mass of the baryon, whereas $E$ is the single particle energy in nuclear matter. Note that

$$E^{*2}=\mathbf{p}^{*2}+M^{*2}\ . \tag{32}$$

It will be useful to introduce the quantities

$$\hat{\mathbf{P}}\equiv\frac{p^*}{E^*}\equiv\cos\eta(p),\quad \hat{M}\equiv\frac{M^*}{E^*}\equiv\sin\eta(p)\ . \tag{33}$$

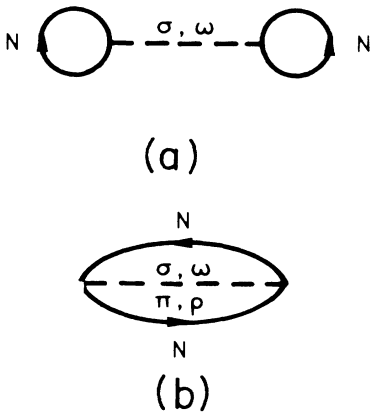


FIG. 2. Diagrammatic representation of the (a) Hartree and (b) Fock contributions to the total binding energy.

The Dirac equation may then be solved formally. The positive energy solution is

$$u(\mathbf{p},s)=\left[\frac{E^*+M^*}{2E^*}\right]^{1/2}\begin{bmatrix}1\\ \dfrac{\boldsymbol{\sigma}\cdot\mathbf{p}^*}{E^*+M^*}\end{bmatrix}\chi_s\ . \tag{34}$$

We have omitted here, for simplicity, the isospin variables. The solution (34) is normalized as

$$u^\dagger(\mathbf{p},s)u(\mathbf{p},s)=1\ . \tag{35}$$

In symmetric ($N=Z$) nuclear matter, the HF trial state is

$$|\phi_0\rangle=\prod_{\mathbf{p},s} b^\dagger(\mathbf{p},s)\,|0\rangle\ , \tag{36}$$

where $|0\rangle$ is the physical vacuum. Using the Hamiltonian derived in Eq. (18), we can calculate the energy density in a given volume $\Omega$:

$$\epsilon=\frac{1}{\Omega}\langle\phi_0|H_0|\phi_0\rangle\equiv\langle T\rangle+\langle V\rangle\ . \tag{37}$$

The kinetic energy $\langle T\rangle$ and the potential energy $\langle V\rangle$ [decomposed into the direct and exchange parts, $\langle V_D\rangle$ and $\langle V_E\rangle$, shown in Figs. 2(a) and 2(b), respectively] depend on the still unknown functions $\hat{M}$ and $\hat{P}$, i.e., on $\eta(p)$, and on the Fermi momentum $p_F$. Their detailed expressions are given in Appendix A. The HF equations are then obtained by requiring that the energy per particle $\epsilon/\rho_B$, where $\rho_B$ is the baryonic density, be stationary with respect to variations of $\rho_B$ and $\eta$. We thus obtain, in the notations of Appendix A:

$$\begin{aligned}&p_F\hat{P}(p_F)+M\hat{M}(p_F)-\left[\frac{g_\sigma}{m_\sigma}\right]^2\rho_S\hat{M}(p_F)+\left[\frac{g_\omega}{m_\omega}\right]^2\rho_B+\frac{1}{(4\pi)^2}\frac{1}{p_F}\\ &\quad\times\int_0^{p_F}p'dp'\{A(p_F,p')+B(p_F,p')\hat{M}(p_F)\hat{M}(p')+C(p_F,p')\hat{P}(p_F)\hat{P}(p')+D(p_F,p')\hat{P}(p_F)\hat{M}(p')\}-\epsilon/\rho_B=0\ ,\end{aligned} \tag{38a}$$

$$-p\hat{M}(p)+M\hat{P}(p)-\left[\frac{g_\sigma}{m_\sigma}\right]^2\rho_s\hat{P}(p)+\frac{1}{(4\pi)^2}\frac{1}{p}\int_0^{p_F}p'dp'\{B(p,p')\hat{P}(p)\hat{M}(p')-C(p,p')\hat{M}(p)\hat{P}(p')$$
$$+\tfrac{1}{2}[D(p',p)\hat{P}(p)\hat{P}(p')-D(p,p')\hat{M}(p)\hat{M}(p')]\}=0\ . \quad (38b)$$

These equations form the basis of our study of nuclear matter. They are solved numerically to yield $\eta(p)$ and the saturation Fermi momentum $p_F^0$. The self-energy $\Sigma(p)$ can then be computed as indicated in Appendix A.

### B. Determination of the parameters

The Lagrangian of the system is entirely determined once the four meson masses and six coupling constants are given. On the other hand, the two basic properties of nuclear matter we have to reproduce are the nuclear binding energy per particle and its saturation density. In order to reduce the number of parameters, we fix the meson masses to their physical values, $m_\omega=783$ MeV, $m_\rho=770$ MeV, and $m_\pi=138$ MeV, while the bare nucleon mass is taken as $M=938.9$ MeV. The mass of the $\sigma$ meson, however, is not fixed since it corresponds to a representation of the two $\pi$-exchange contribution. It should lie between 400 and 600 MeV, according to the construction of the NN potential.

For the coupling constants, we fix the $\pi$-N and $\rho$-N coupling constants to their well-known physical values, namely $f_\pi^2/4\pi=0.08$ and $g_\rho^2/4\pi=0.55$. The tensor $\rho$-N coupling constant is related to the ratio $f_\rho/g_\rho$. When the vector dominance model is assumed, its value is identified to the isovector anomalous magnetic moment (in Bohr magnetons) of the nucleon, that if $f_\rho/g_\rho\equiv\kappa_v=\mu_p-\mu_n-1=3.7$. However, it has been shown long ago that a larger value is needed to understand $\pi$N-scattering data, namely $f_\rho/g_\rho=6.6$. Since the HF approximation tends to overestimate the short-range contributions (the total energy is calculated with uncorrelated wave functions), we expect that the use of the smaller value of $f_\rho$ in the HF approximation will somehow simulate a more realistic calculation made with the larger value of it. On the other hand, the tensor $\omega$-N coupling constant is related to the isoscalar anomalous magnetic moment of the nucleon, $f_\omega/g_\omega\equiv\kappa_s=\mu_p+\mu_n-1=-0.12$. This value is quite small, and therefore we shall neglect it in the present numerical calculations. Note, however, that this term is of great importance when the present scheme is extended to hypernuclei since at one vertex the meson-nucleon coupling constants have to be replaced by the meson-hyperon ones. Since the ratio $f_\omega/g_\omega$ for a hyperon is quite large, it cannot be neglected. This term is indeed essential to get the right value for the observed spin-orbit splitting in hypernuclei.[20]

Therefore, there are only three adjustable parameters in our scheme, the $\sigma$- and $\omega$-nucleon coupling constants and the $\sigma$-meson mass. For all the results we shall present, these are chosen to reproduce the empirical saturation point of nuclear matter, $E/A=\epsilon/\rho_B-M=-15.75$ MeV and $p_F^0=1.30$ fm$^{-1}$ ($\rho^0=0.1484$ fm$^{-3}$). The $\sigma$-meson mass is adjusted to get the right charge rms radius for $^{16}$O and is taken to be $m_\sigma=440$ MeV (see Sec. IV for more details). Finally, in order to be consistent with our description in terms of a *local* Lagrangian density, no form factors have been used at the meson-nucleon vertices (no divergences occur in the HF approximation). In the limit of large cutoff masses for $\pi$- and $\rho$-exchange potentials (larger than 1300 MeV for $\pi$ and 1500 MeV for $\rho$ contributions), this should be a reasonable approximation. For $\sigma$- and $\omega$-exchange contributions, all finite size effects are expected to be included in the fitted coupling constants. The $\delta(\mathbf{r})$ part of the $\pi$- and $\rho$-induced interactions has been removed from the Hamiltonian used throughout this work (see Ref. 21 for results which include these contributions).

### C. Numerical results and discussion

Some of the nuclear matter results presented here are already known,[10,11] but we show them again for a comparison with complete calculations including all four mesons. The parameters of the model are given in Table I for different cases of interest in the Hartree or Hartree-Fock approximation. If the model is restricted first to the isoscalar mesons only [rows (a) and (b)], the coupling constants have to be renormalized by 15—20% when going from the Hartree to the HF approximation. Indeed, without this renormalization one would get too little binding in the HF approximation, as one can see in Fig. 3. Furthermore, the net contribution of $\pi$ and $\rho$ exchange is obvious on this figure (dashed-dotted line) when the isoscalar meson coupling constants are kept fixed. One gains in that case about 20 MeV per nucleon of attraction.

Since the pv $\pi$-N coupling constant is much weaker than the scalar and vector couplings, $g_\sigma$ and $g_\omega$ have to be only slightly renormalized to get the saturation point of nuclear matter when the pion exchange contribution is taken into account, as can be seen from row (c) of Table I.

TABLE I. Isoscalar scalar ($\sigma$) and vector ($\omega$) meson coupling constants determined by adjusting the saturation point of infinite nuclear matter, for Hartree ($H$) and Hartree-Fock (HF) approximations. The isovector meson coupling constants are explained in the text. Rows (d) and (e) correspond to $f_\rho/g_\rho=6.6$ and 3.7, respectively. All results correspond to $m_\sigma=440$ MeV.

| | $g_\sigma^2/4\pi$ | $g_\omega^2/4\pi$ |
|---|---|---|
| (a) $(\sigma+\omega)_H$ | 6.25 | 15.16 |
| (b) $(\sigma+\omega)_{HF}$ | 5.54 | 12.24 |
| (c) $(\sigma+\omega+\pi)_{HF}$ | 5.35 | 12.42 |
| (d) $(\sigma+\omega+\pi+\rho)_{HF}$ $\kappa=6.6$ | 2.27 | 10.00 |
| (e) $(\sigma+\omega+\pi+\rho)_{HF}$ $\kappa=3.7$ | 4.16 | 11.18 |

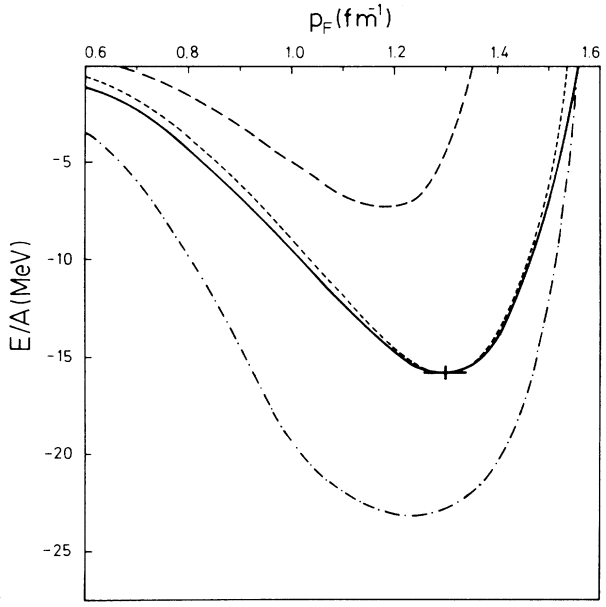


FIG. 3. Binding energies per particle in infinite nuclear matter. The short-dashed curve corresponds to the Hartree approximation with parameter set (a) of Table I. The solid curve is calculated with the parameter set (e) (HF approximation with all mesons included). The long-dashed curve corresponds to the HF approximation with the parameters of row (a) and $\sigma,\omega$ mesons only. The dashed-dotted curve is calculated in the HF approximation with all mesons included and parameter set (a).

The $\rho$-meson contribution is divided into three different parts: a vector part proportional to $g_\rho^2$, a tensor part proportional to $f_\rho^2$, and a cross vector-tensor part proportional to $f_\rho g_\rho$. The net effect of the $\rho$ meson with a tensor coupling given by $f_\rho/g_\rho=3.7$ is attractive and of the order of 19 MeV/nucleon in nuclear matter. This leads to the new values of $g_\sigma$ and $g_\omega$ shown in row (e) of Table I.

### 1. Kinetic and potential energies

Here we examine how the total energy per particle is divided into kinetic energy and potential energies due to the various mesons. In the nonrelativistic case the kinetic energy operator is defined as the part of the Hamiltonian which remains in the limit of vanishing interactions. We take the same definition in the relativistic case [see Eqs. (18)–(20)]. In both cases the rest mass is subtracted out. In Table II are shown the kinetic energy $T^R=\langle T\rangle/\rho_B-M$, and the direct and exchange potential energies for each meson. They have been obtained with the parameter sets of Table I.

It is remarkable that $T^R$ is always smaller than $T^{\rm NR}=\frac{3}{10}(p_F^2/M)$, the nonrelativistic kinetic energy. It can easily be shown in the Hartree approximation that, to first order in a low density expansion,

$$T^R\simeq T^{\rm NR}\left[1-\frac{1}{M}\left[\frac{g_\sigma}{m_\sigma}\right]^2\rho_B\right]. \tag{39}$$

At saturation density, $T^{\rm NR}$ is about 21 MeV for $p_F^0=1.30$ fm$^{-1}$, while the values of $T^R$ shown in Table II range from $\frac{1}{2}$ of $\frac{1}{4}$ of $T^{\rm NR}$. This small value of $T^R$ helps to get the correct binding energy in finite nuclei without requiring very deep single particle energies (see Sec. IV).

As for the potential energies, it is well known [see, e.g., Eq. (A3) of Appendix A] that in the $(\sigma,\omega)$ Hartree approximation the potential energy results from a balance between two large numbers, namely a strong attractive contribution from $\sigma$ exchange and a strong repulsive part from $\omega$ exchange. In the $(\sigma,\omega)$ HF approximation, the $\sigma$ and $\omega$ net contributions become, respectively, much less attractive and repulsive. Furthermore, when other mesons are taken into account, the attraction is shared between the $\sigma$ meson and the isovector $\pi$ and $\rho$ mesons, while the repulsion due to the $\omega$ meson is reduced by roughly one-third. The cancellations between various mesons are therefore less extreme in the HF approximation than in the Hartree one. Nevertheless, the different potential energies are still large. In the HF case the total contribution of isoscalar mesons to the binding energy is surprisingly small (0.5 MeV, see Table II). This (almost exact) cancellation even persists in finite nuclei. This does not mean obviously that $\sigma$ and $\omega$ mesons play no role in the saturation mechanism. Indeed, self-consistency effects are important, for a correct calculation of $\sigma$ and $\omega$ contributions.

### 2. Bulk properties

In Table III is shown the compression modulus $K$ corresponding to the various cases of Table I. One sees that in the $(\sigma,\omega)$ model the Fock terms increase $K$ by roughly 10%, but the addition of the pion brings it to its initial value. The effect of the $\rho$ meson is to lower $K$ by about 20%. This is mainly attributed to the tensor part of the $\rho$-nucleon coupling. A larger value of $f_\rho$ [row (d)] leads

TABLE II. Kinetic and potential energies per particle for the parameter sets of Table I. All quantities are in MeV.

| | $T^R$ | $\langle V_D\rangle/\rho_B$ | | $\langle V_E\rangle/\rho_B$ | | | |
|---|---|---|---|---|---|---|---|
| | | $\sigma$ | $\omega$ | $\sigma$ | $\omega$ | $\pi$ | $\rho$ |
| (a) | 8.1 | −201 | 177 | | | | |
| (b) | 5.2 | −176 | 143 | 35 | −23 | | |
| (c) | 7.1 | −171 | 145 | 34 | −24 | −6.7 | |
| (d) | 13.1 | −75 | 117 | 15 | −21 | −6.5 | −58 |
| (e) | 9.2 | −135 | 131 | 26 | −22 | −6.6 | −19 |

TABLE III. Compression modulus $K$, symmetry energy $a_4$, effective mass $M^*/M$ at $p_F=p_F^0$, and mean velocity $\langle v/c \rangle$ calculated with the parameter sets of Table I.

| | $K$ (MeV) | $a_4$ (MeV) | $M^*/M$ | $\langle v/c \rangle$ |
|---|---|---|---|---|
| (a) | 540 | 19.5 | 0.54 | 0.35 |
| (b) | 615 | 29.5 | 0.51 | 0.30 |
| (c) | 545 | 29.5 | 0.51 | 0.33 |
| (d) | 355 | 28 | 0.63 | 0.42 |
| (e) | 465 | 28 | 0.56 | 0.37 |

to a smaller value of $K$. In any case, the compression modulus is larger than the currently accepted value ($K=210$ MeV). This could result in important implications for the study of finite nuclei. However, it is rather satisfactory that the most complete calculation including isoscalar and isovector mesons gives the smaller value of $K$. Furthermore, it is expected that going beyond the HF approximation (taking into account correlations for instance) will also reduce the compression modulus.

Also given in Table III is the bulk symmetry energy coefficient $a_4$. The contribution from the Fock terms can easily be evaluated in the following approximation. The isoscalar contributions are proportional to

$$N^2+Z^2=\frac{A^2}{2}\left[1+\left[\frac{N-Z}{A}\right]^2\right],$$

where $N$ and $Z$ are the numbers of neutrons and protons, respectively. Then, the contribution to the symmetry energy coefficient coming from isoscalar mesons is equal to their potential energy in symmetric matter. For isovector mesons, the contribution to the energy is proportional to

$$\sum_{q_a,q_b}\langle q_a,q_b \mid \tau_1\cdot\tau_2 \mid q_b,q_a\rangle = N^2+4NZ+Z^2 = \frac{3A^2}{2}\left[1-\frac{1}{3}\left[\frac{N-Z}{A}\right]^2\right],$$

so that the contribution to $a_4$ coming from isovector mesons is equal to one-third of the corresponding potential energy with an opposite sign. The contributions from kinetic and direct potential energies are evaluated numerically. Fock terms are essential in getting the right order of magnitude for $a_4$, which is empirically about 33 MeV. There is, therefore, no need to use a large value of the isovector-vector coupling constant $g_\rho$, as is usually done in Hartree calculations of finite nuclei.

All the results we have discussed are based on a fixed value of the scalar mass, $m_\sigma=440$ MeV. It is known [see Eqs. (38)] that, in the Hartree approximation, the results depend only on the ratios $(g_\sigma/m_\sigma)^2$ and $(g_\omega/m_\omega)^2$, but it is not strictly so in the HF approximation. However, as noticed already in Ref. 11, a reasonable variation in $m_\sigma$ entails only very small changes in the ratio $(g_\sigma/m_\sigma)^2$. Note that the ratio $(g_\omega/m_\omega)^2$ is also slightly changed due to the effect of self-consistency. Consequently, once $(g_\sigma/m_\sigma)$ is fixed, varying $m_\sigma$ has only little influence on the bulk properties of nuclear matter. On the other hand, finite nuclei are more affected by the value of $m_\sigma$ since it sets the scale of the intermediate range attraction and thus influences properties like the rms radii.

### 3. *Baryon self-energies and energy spectrum*

We come now to the discussion of the different components of the baryon self-energy $\Sigma$. In the Hartree approximation, the scalar component $\Sigma_S$ is entirely given by the scalar $\sigma$ meson, the time component $\Sigma_0$ of the vector part comes from the vector $\omega$ meson, while the space component $\Sigma_V$ is identically zero. This is not the case in the HF approximation, where both $\sigma$ and $\omega$ (time *and* space parts) mesons contribute to the three components. In addition, the three self-energies receive contributions from $\pi$ and $\rho$ isovector mesons. The self-energies calculated at saturation density are shown in Table IV.

The functions $\Sigma_S$ and $\Sigma_0$ depend very little on momentum, as shown in Fig. 4, where the calculations have been performed with the parameter set (e) of Table I (note that these functions are momentum independent in the Hartree approximation). They can be approximated by the following parametrization:

$$\Sigma_S(p)=-(325+100e^{-p^2/m^2})\ \text{MeV}\ ,\qquad \Sigma_0(p)=(265+80e^{-p^2/m^2})\ \text{MeV}\ , \tag{40}$$

with $m=783$ MeV. On the contrary, the component $\Sigma_V$ has a stronger momentum dependence, as can be seen from Fig. 4. The value of $\Sigma_V$ comes almost entirely from

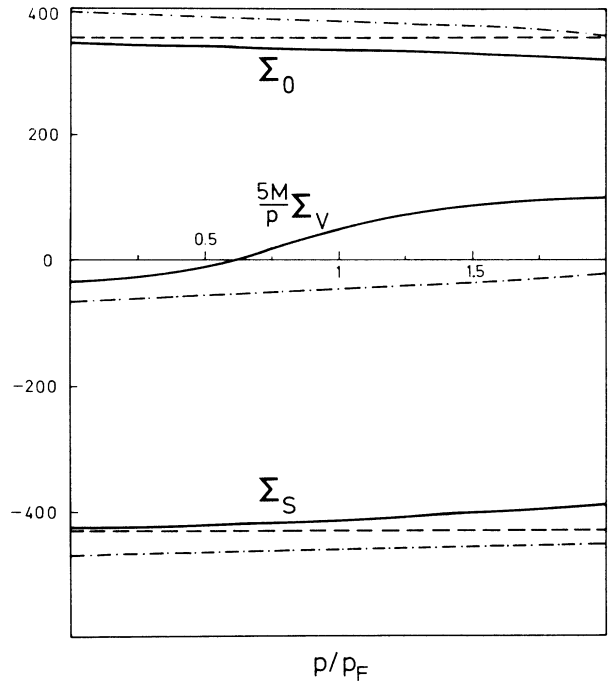


FIG. 4. Components of the baryon self-energy in MeV. The dashed and solid curves correspond, respectively, to the Hartree approximation [row (a) of Table I] and the HF approximation [row (e)]. The dashed-dotted lines correspond to the HF approximation with $\sigma$ and $\omega$ mesons only. The vector component $\Sigma_V$ has been multiplied for convenience by a factor $5M/p$.

TABLE IV. Components of the baryon self-energy $\Sigma$ (in MeV) calculated at saturation density, with parameter set (e) of Table I. The values obtained in the Hartree approximation with parameter set (a) are also shown .

| | | $\Sigma_S$ | $\Sigma_0$ | $\Sigma_V$ |
|---|---|---|---|---|
| Direct | | −288 ($\sigma$) | 261 ($\omega$) | 0 |
| Exchange | $\sigma$ | 24 | 26 | −1 |
| | $\omega$ | −105 | 56 | −1 |
| | $\pi$ | −5 | −5 | −6 |
| | $\rho$ | −40 | −1 | 11 |
| Total (e) | | −414 | 337 | 3 |
| Hartree (a) | | −431 | 354 | 0 |

the contributions of $\pi$ and $\rho$ mesons, with opposite signs, the cross vector-tensor term giving the largest contribution. Isoscalar $\sigma$ and $\omega$ mesons give at most (near the saturation point) −1 MeV each. It is remarkable that $\Sigma_V$ is very small as compared to $\Sigma_S$ and $\Sigma_0$. Actually, we can see from the definition (31) that the effective momentum $\mathbf{p}^*$ in nuclear matter is very close to the free momentum $\mathbf{p}$, the difference at saturation density being of the order of 5%. However, some caution is necessary when comparing the value of the self-energy $\Sigma_V$ from different authors, since there are different ways to carry a Lorentz decomposition of the baryon self-energy $\Sigma$. Our choice was to start with the expression (29) satisfying the Dirac equation (30). But, as shown in Ref. 22, the quantity $\Sigma_V$ can also be eliminated in the Dirac equation in nuclear matter, resulting in new, energy dependent self-energies $\Sigma_S$ and $\Sigma_0$. We note that our values for the latter are within 10% of those given in Refs. 12 and 13, where a different approach is used. In these references one starts with a relativistic Brueckner-Hartree-Fock treatment of nuclear matter based on a OBEP (one-boson exchange potential) which fits NN-phase shifts. While the self-energies are similar in both approaches, our effective coupling constants are different, especially for the $\omega$ meson (see discussion in Sec. II E).

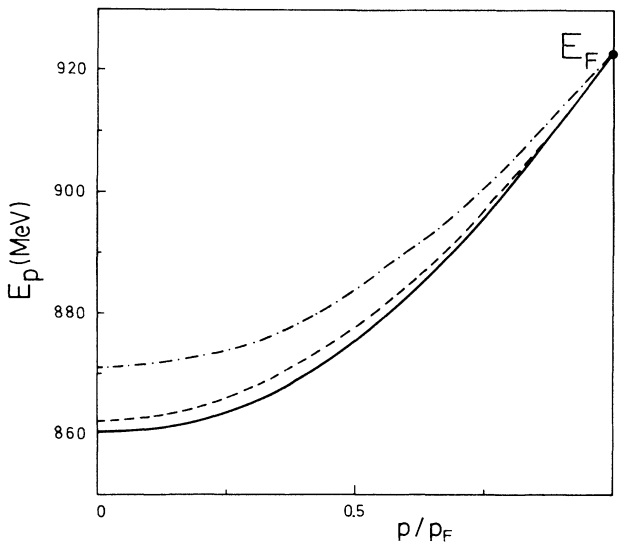


FIG. 5. Single-particle energy spectrum in nuclear matter. The dashed curve corresponds to the Hartree approximation [row (a) of Table I]. The other curves are calculated in the HF approximation: solid, (e); dashed-dotted, (b).

The single particle energy spectrum is given by the dispersion relation (32). The values of $E(p)$ are represented in Fig. 5 for different cases of interest. Since the models are adjusted to the saturation point of nuclear matter, all curves must reach the same point at $p=p_F^0$, where the energy is equal to the Fermi energy $E_F=M-15.75$ MeV. First, one notes that at $p=0$ the nucleons are less bound in the HF approximation than in the Hartree one when the calculations are restricted to isoscalar mesons only. They are, however, slightly more bound when isovector mesons are taken into account. For small values of the momentum, the net effect of the latter is of the order of 2 MeV for parameter set (e) [12 MeV for set (d)]. One also sees that the slopes of the different curves near the Fermi surface are different, i.e., the density of states is different, depending on which mesons are included in the HF approximation. The density of states is largest in the case where all mesons are included.

### D. Nucleon effective mass

The scalar self-energy $\Sigma_S$ modifies the baryon mass in matter from its bare value $M$ to an effective value $M^*(p)$ as shown in Eq. (31). This scalar effective mass determines the ratio of the upper to the lower component of the baryon spinor. The calculated values of $M^*(p=p_F^0)$ are shown in Table III. They are roughly half the free baryon mass, although the inclusion of isovector mesons (especially the tensor part of the $\rho$ meson) tends to increase them by 10—20%.

In nonrelativistic theories, one introduces an effective mass $M^*_{\rm NR}$ obeying the relation

$$M^*_{\rm NR}(p)=p\left[\frac{dE_{\rm NR}}{dp}\right]^{-1}, \tag{41}$$

where $E_{\rm NR}$ is the nonrelativistic energy of the particle. For a free particle, $M^*_{\rm NR}$ is equal to $M$, as it should, and in the general case it is proportional to the density of single particle states. Usual HF or BHF calculations give $M^*_{\rm NR}(p_F^0)\simeq 0.7M$. This is an overly low value compared to phenomenology, the well known reason being the neglect in these models of dynamical effects leading to an explicit energy dependence of the nuclear potential. Of course, the present HF calculations suffer the same defect. Nevertheless, it is possible to compare the density of states predicted by a relativistic and a nonrelativistic HF model. To this end, it is convenient to use the relativistic generalization of (41) proposed in Ref. 11:

$$\tilde{M}(p)=p\left[\left[\frac{dE}{dp}\right]^{-2}-1\right]^{1/2}, \tag{42}$$

where $E$ is the total relativistic energy of the particle. For a free particle one again has $\tilde{M}=M$, and in the general

case the density of states is proportional to $[\widetilde{M}^2(p)+\mathbf{p}^2]^{1/2}$. It is easily seen that the relation between $\widetilde{M}$ and $M^*$ is

$$\widetilde{M}(p)=M^*(p)\frac{[1-\Delta(\Delta+2p^*)/M^{*2}]^{1/2}}{1+(\Sigma_V+\Delta)/p} , \tag{43}$$

where

$$\Delta=p^*\frac{d\Sigma_V}{dp}+M^*\frac{d\Sigma_S}{dp}+E^*\frac{d\Sigma_0}{dp} .$$

In the Hartree approximation, both $\Sigma_V$ and $\Delta$ are identically zero; $\widetilde{M}$ and $M^*$ are the same and they do not depend on momentum. In the HF approximation, however, they will differ. For instance, when all mesons are included [parameter set (e)], $\widetilde{M}(p_F^0)$ is approximately 10% smaller than $M^*(p_F^0)$. To make the connection with the nonrelativistic definition of the effective mass clearer, we recall that in the case of the Skyrme interaction the effective mass comes from the momentum dependent part of the energy functional. In nuclear matter its contribution to the binding energy is approximately equal to $7(\rho/\rho_0)^{5/3}$ MeV for the Skyrme III interaction. In the relativistic approach the momentum dependence comes first from kinematical corrections due to the small component of the nucleon spinor, and second from the further modification of this component due to dynamical effects. The first type of correction also gives a $\rho^{5/3}$ density dependence. This establishes the connection between the Skyrme HF approach and the present one.

### E. Saturation mechanism

The saturation mechanism in such a relativistic scheme can be understood by looking at different approximations of the complete, self-consistent model. Let us first estimate the average velocity of the nucleons in the medium. The nucleon velocity is defined as the derivative of the single particle energy with respect to the momentum. In the Hartree approximation, for instance, the average velocity is just

$$\left\langle\frac{v}{c}\right\rangle=\frac{2}{\pi^2}\int_0^{p_F}p^2dp\frac{p}{(\mathbf{p}^2+M^{*2})^{1/2}}\simeq\frac{3}{2}\frac{p_F}{M^*} , \tag{44}$$

the last equality being obtained in a low density expansion. The exact numerical values given in Table III are larger than in nonrelativistic models, where $\langle v/c\rangle\simeq 0.25$. Such numbers indicate that one can expect corrections at least of the order of a few MeV ($\sim\frac{1}{2}(v^2/c^2)\Sigma_0$) at normal nuclear density.

In order to get simple analytical expressions, we shall discuss here the $(\sigma,\omega)$ model in the Hartree approximation. In this case, the self-consistency condition (38b) becomes

$$M^*-M=\Sigma_S=-\left[\frac{g_\sigma}{m_\sigma}\right]^2\rho_S , \tag{45}$$

while the binding energy per particle is

$$\frac{\epsilon}{\rho_B}-M=\frac{1}{2}\left[\frac{g_\omega}{m_\omega}\right]^2\rho_B-\frac{1}{2}\left[\frac{g_\sigma}{m_\sigma}\right]^2\frac{\rho_S^2}{\rho_B}+\frac{2}{\pi^2}\frac{1}{\rho_B}\int_0^{p_F}p^2dp(p\hat{P}+M\hat{M})-M . \tag{46}$$

For large values of $p_F$ (i.e., large densities) the effective mass goes to zero as $1/p_F^2$ while the scalar density $\rho_s$ goes to a finite value, contrary to the baryonic density $\rho_B$, which increases as $p_F^3$. The saturation curve is dominated at large $p_F$ by $\omega$ exchange, while at low density the kinetic term is dominating. It is the delicate balance between the attractive $\sigma$- and repulsive $\omega$-meson contribution which gives the nuclear binding at $p_F=p_F^0$.

It is interesting to examine how different approximations affect the saturation mechanism. The Dirac spinor of the dressed nucleon can be exactly decomposed[12,23] on the basis of free particle and antiparticle Dirac spinors, $u^0(\mathbf{p},s)$ and $v^0(\mathbf{p},s)$. One gets

$$u(\mathbf{p},s)=\frac{1}{[1+\alpha^2(p)]^{1/2}}[u^0(\mathbf{p},s)+\alpha(p)\sum_{s'}\langle s\,|\,\boldsymbol{\sigma}\cdot\hat{\mathbf{p}}\,|\,s'\rangle\times v^0(-\mathbf{p},-s')] . \tag{47}$$

For $p/M^*\ll 1$, $\alpha(p)$ is given approximately by

$$\alpha(p)\simeq\frac{p(M-M^*)}{2MM^*} , \tag{48}$$

which is at most of the order of 0.10 at $p_F=p_F^0$.

The first approximation consists of neglecting $\alpha(p)$ in Eq. (47) and replacing $M^*$ by $M$ in the energy functional (42), i.e., one approximates $\hat{P}$ and $\hat{M}$ by

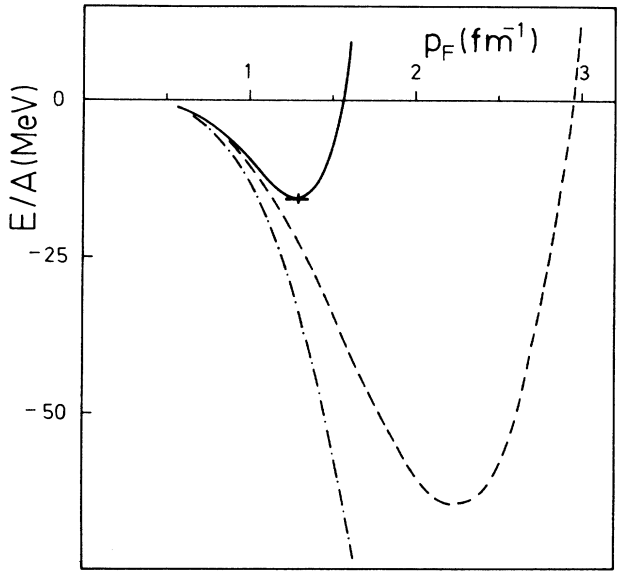


FIG. 6. Different approximations to the binding energy per particle in infinite nuclear matter for parameter set (e). The solid line corresponds to the complete, self-consistent calculation. The dashed line corresponds to the replacement of the Dirac spinors in the medium by the free ones. The dashed-dotted curve is the result of a nonrelativistic expansion ($p\ll M$) of the binding energy.

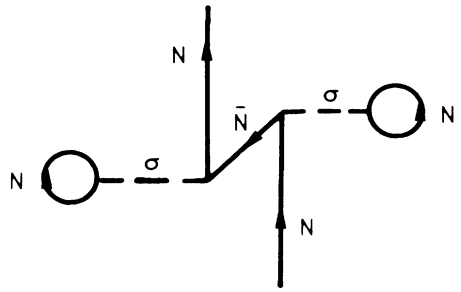


FIG. 7. First order contribution to the nucleon wave function in a relativistic expansion in $\alpha(p)$ [see Eq. (47)].

$$\hat{P}=\frac{p}{(\mathbf{p}^2+M^2)^{1/2}},\quad \hat{M}=\frac{M}{(\mathbf{p}^2+M^2)^{1/2}}\ . \tag{49}$$

In this case the saturation energy curve is given by the dashed line in Fig. 6. The correction is of the order of 8 MeV at the saturation point $p_F=p_F^0$. This indicates that the contribution of the free negative energy component in the dressed Dirac spinor is repulsive and quite large.

In first order perturbation theory, corrections to the nucleon wave function[24] coming from the negative energy solution of the free Dirac equation are rendered pictorially in Fig. 7. This gives rise explicitly to the modification of the lower component of the free nucleon spinor by a factor $M/M^*=1-\Sigma_S/M$ in first order. One interesting result is that the contribution of such a process to the binding energy is of the order of $5(\rho/\rho_0)^{8/3}$ MeV. This type of contribution to the effective mass could be simulated by a generalized Skyrme interaction containing velocity-density—dependent terms.

Finally, the strictly nonrelativistic limit, with no relativistic kinematical corrections, consisting of dropping terms in $p/M$ as compared to 1 in the energy functional, or equivalently by setting $\hat{P}=0$ and $\hat{M}=1$ in the potential energy, gives no saturation at all for the particular set of parameters we took [set (e) of Table I]. The relativistic kinematical corrections amount to about 10 MeV repulsion at normal nuclear density (see Fig. 6). This means that at least these corrections ("minimal relativity") are essential to get the saturation point in the HF approximation, and for the two body interactions considered in this work.

## IV. FINITE NUCLEI

### A. The Hartree-Fock equations

We now consider the case of spherical, closed-subshell nuclei. In the same way as for infinite nuclear matter, the HF energy is calculated in the tree approximation. The nucleon field is therefore expanded as in Eq. (17) without the $d$ and $d^\dagger$ terms. A single-particle baryon state with energy $E_\alpha$ is specified by the set of quantum numbers $\alpha=(q_a,n_a,l_a,j_a,m_a)\equiv(a,m_a)$, where $q_a=-1$ for a neutron state and $q_a=+1$ for a proton state. The baryon spinor $f_\alpha(\mathbf{r})$ is written explicitly as

$$f_\alpha(\mathbf{r})=\frac{1}{r}\begin{bmatrix} iG_a(r) \\ F_a(r)\boldsymbol{\sigma}\cdot\hat{\mathbf{r}}\end{bmatrix}\mathcal{Y}_\alpha(\hat{\mathbf{r}})\chi_{1/2}(q_a)\ , \tag{50}$$

where $\chi_{1/2}(q_a)$ is an isospinor, and

$$\mathcal{Y}_\alpha(\hat{\mathbf{r}})=\sum_{\mu_a,s_a}(l_a\ \tfrac{1}{2}\ \mu_a\ s_a\mid j_a\ m_a)Y_{l_a}^{\mu_a}(\hat{\mathbf{r}})\chi_{1/2}(s_a)\ . \tag{51}$$

The spinors $f_\alpha$ are normalized according to

$$\int d^3r\, f_\alpha^\dagger(\mathbf{r})f_\alpha(\mathbf{r})=\int_0^\infty [G_a^2(r)+F_a^2(r)]dr=1\ . \tag{52}$$

In the $\{\alpha\}$ representation, the kinetic and interaction parts of the Hamiltonian (18), in the static approximation, are

$$\begin{aligned} T&=\sum_{\alpha\beta}b_\alpha^\dagger b_\beta\int d^3r\,\bar{f}_\alpha(\mathbf{r})(-i\boldsymbol{\gamma}\cdot\boldsymbol{\nabla}+M)f_\beta(\mathbf{r})\ , \\ V_i&=\tfrac{1}{2}\sum_{\substack{\alpha\beta\\ \gamma\delta}}b_\alpha^\dagger b_\beta^\dagger b_\gamma b_\delta(\text{isospin}) \\ &\quad\times\int d^3r_1d^3r_2\bar{f}_\alpha(\mathbf{r}_1)\bar{f}_\beta(\mathbf{r}_2)[\Gamma_i(1,2)v(m_i;1,2)] \\ &\quad\times f_\gamma(\mathbf{r}_2)f_\delta(\mathbf{r}_1)\ , \end{aligned} \tag{53}$$

where the $v$'s are Yukawa factors:

$$v(m;1,2)=\frac{1}{4\pi}\frac{e^{-m\mid\mathbf{r}_1-\mathbf{r}_2\mid}}{\mid\mathbf{r}_1-\mathbf{r}_2\mid}\ . \tag{54}$$

The shorthand notation for isospin is the same as in Eq. (20). The various quantities $\Gamma_i(1,2)$ expressed in coordinate space are listed below, when they are different from those given in Eq. (21):

$$\begin{aligned} \Gamma_\pi^{\text{pv}}(1,2)&=-\left[\frac{f_\pi}{m_\pi}\right]^2(\gamma_5\gamma^k)_1(\gamma_5\gamma^l)_2\partial_k(1)\partial^l(2)\ , \\ \Gamma_\rho^T(1,2)&=\left[\frac{f_\rho}{2M}\right]^2\sigma_{\nu k}(1)\sigma^{\nu l}(2)\partial^k(1)\partial_l(2)\ , \\ \Gamma_\rho^{VT}(1,2)&=\left[\frac{f_\rho g_\rho}{2M}\right][\sigma^{k\nu}(1)\gamma_\nu(2)\partial_k(1) \\ &\quad+\gamma_\nu(1)\sigma^{k\nu}(2)\partial_k(2)]\ . \end{aligned} \tag{55}$$

In keeping with the approximations already used in infinite nuclear matter, we neglected in these expressions the retardation effects which cause a state dependence in the interactions. According to the discussion in Sec. II E, we also subtracted from the Hamiltonian the zero-range interactions which are contained in $\Gamma_\pi$ and $\Gamma_\rho^T$. This is done, according to the prescription (28), by adding the two terms:

$$\begin{aligned} &\delta[\Gamma_\pi^{\text{pv}}v(m_\pi;1,2)] \\ &\quad=\frac{1}{3}\left[\frac{f_\pi}{m_\pi}\right]^2\boldsymbol{\gamma}(1)\cdot\boldsymbol{\gamma}(2)\gamma_5(1)\gamma_5(2)\delta(\mathbf{r}_1-\mathbf{r}_2)\ , \\ &\delta[\Gamma_\rho^Tv(m_\rho;1,2)]=\frac{1}{3}\left[\frac{f_\rho}{2M}\right]^2\sigma^{\mu i}(1)\sigma_{\mu i}(2)\delta(\mathbf{r}_1-\mathbf{r}_2)\ . \end{aligned} \tag{56}$$

We now consider a nucleus with $A$ nucleons. In the HF approximation, the trial ground state is

$$\mid\phi_0\rangle=\prod_{\alpha\ (\text{occupied})}b_\alpha^\dagger\mid 0\rangle\ . \tag{57}$$

The HF solution is obtained by requiring that the total binding energy,

$$E=\langle\phi_0\,|\,H_0\,|\,\phi_0\rangle-AM\ , \tag{58}$$

be stationary with respect to variations of the spinors $f_\alpha$ (i.e., of $G_a$ and $F_a$) such that the normalization relation (52) is preserved. This is expressed as usual by the condition

$$\delta\left[E-\sum_{\alpha\ (\text{occupied})}E_\alpha\int f_\alpha^\dagger(\mathbf{r})f_\alpha(\mathbf{r})d^3r\right]=0\ , \tag{59}$$

where the $E_\alpha$ are Lagrange multipliers. It will turn out that the $E_\alpha$ are just the HF single particle energies (including nucleon mass). The calculation of $\langle\phi_0\,|\,H_0\,|\,\phi_0\rangle$ is very lengthy and it will not be detailed here. It requires a great deal of care, but otherwise presents no special difficulty. We have checked our general expressions in two limiting cases where the results are relatively simple, first by considering the $^4$He nucleus and, second, in the limit of infinite meson masses (zero-range approximation). Once $\langle\phi_0\,|\,H_0\,|\,\phi_0\rangle$ is calculated, one can perform the variations (59) and then obtain the HF equations for the self-consistent wave functions $(G_a,F_a)$ and energies $E_a$. They take the following form:

$$\frac{d}{dr}\begin{bmatrix}G_a(r)\\F_a(r)\end{bmatrix}=\begin{bmatrix}-\frac{\kappa_a}{r}-\Sigma_{T,a}^D(r) & M+E_a+\Sigma_{S,a}^D(r)-\Sigma_{0,a}^D(r)\\ M-E_a+\Sigma_{S,a}^D(r)+\Sigma_{0,a}^D(r) & \frac{\kappa_a}{r}+\Sigma_{T,a}^D(r)\end{bmatrix}\begin{bmatrix}G_a(r)\\F_a(r)\end{bmatrix}+\begin{bmatrix}-X_a(r)\\Y_a(r)\end{bmatrix}\ . \tag{60}$$

Here, $\Sigma_{S,a}^D$, $\Sigma_{0,a}^D$, and $\Sigma_{T,a}^D$ are direct contributions to the self-energy, whereas $X_a$ and $Y_a$ come from exchange (Fock) contributions. The quantity $\kappa_a$ is $(2j_a+1)(l_a-j_a)$. The direct potentials are local and state independent. The detailed expressions for all potentials are given in Appendix B.

The HF binding energy of Eq. (58) satisfies the relation

$$E=\tfrac{1}{2}\sum_{\alpha\ (\text{occupied})}(T_\alpha+E_\alpha)-AM\ , \tag{61}$$

where $T_\alpha$ is the kinetic energy of the orbital $\alpha$:

$$T_\alpha=\int d^3r\,\bar{f}_\alpha(\mathbf{r})(-i\boldsymbol{\gamma}\cdot\boldsymbol{\nabla}+M)f_\alpha(\mathbf{r})\ . \tag{62}$$

The relation (61) can be used, in principle, as a check of self-consistency. In our numerical calculations we find, however, that approximate equality between the right-hand sides of Eqs. (58) and (61) does not always ensure that a self-consistent solution has been reached. Details on the numerical procedure for solving the HF equations (60) are given in Appendix C.

### B. Ground state properties

We now present results for ground state properties of some closed shell nuclei, namely the binding energy per particle, rms charge radius, and the proton spin-orbit splitting for the $1p$ shell in $^{16}$O and the $1d$ shell in $^{40}$Ca and $^{48}$Ca. These results are shown in Tables V and VI. The calculations have been done with the various parameter sets of Table I. As we have already mentioned in our discussion of nuclear matter, the properties of finite nuclei are sensitive to the value of the scalar meson mass $m_\sigma$ once the other meson masses are kept fixed, because $m_\sigma$ sets the intermediate range attraction and thus influences rms radii. Our point of view is to choose a value of $m_\sigma$ which gives the most reasonable results for the case we consider to be the most realistic (all mesons included, and $f_\rho/g_\rho=3.7$). We find that the appropriate choice is $m_\sigma=440$ MeV. By using the same value of $m_\sigma$ for all the parameter sets, one can see more clearly the effects of adding more mesons or changing the $\rho$ tensor-coupling strength.

Inclusion of Fock terms in the $(\sigma,\omega)$ model slightly increases the binding energy and consequently decreases the rms radius, but has a dramatic effect on the spin-orbit splitting, which is then too large, especially for $^{48}$Ca.

It is the role of the pion to lower appreciably the spin-orbit splitting while leaving the binding energy and rms radius at the level of the $(\sigma,\omega)$ Hartree approximation. This point is particularly striking when looking at $^{48}$Ca,

TABLE V. Bulk properties of some finite nuclei calculated with the parameter sets of Table I. The total binding energies per particle and the proton spin-orbit splitting for the $1p$ shell ($^{16}$O) or $1d$ shell ($^{40}$Ca and $^{48}$Ca) are given in MeV; the rms charge radii are in fm.

| | $^{16}$O | | | $^{40}$Ca | | | $^{48}$Ca | | |
|---|---|---|---|---|---|---|---|---|---|
| | $-E/A$ | $r_c$ | $\Delta_{LS}$ | $-E/A$ | $r_c$ | $\Delta_{LS}$ | $-E/A$ | $r_c$ | $\Delta_{LS}$ |
| (a) | 2.04 | 3.07 | 4.1 | 4.06 | 3.70 | 5.9 | 4.61 | 3.67 | 6.2 |
| (b) | 2.33 | 2.93 | 7.1 | 4.32 | 3.59 | 8.6 | 5.04 | 3.56 | 8.9 |
| (c) | 3.09 | 2.91 | 5.5 | 4.90 | 3.59 | 7.1 | 5.35 | 3.57 | 3.5 |
| (d) | 11.94 | 2.40 | 9.5 | 11.15 | 3.21 | 8.9 | 11.42 | 3.24 | 1.8 |
| (e) | 5.61 | 2.73 | 7.3 | 6.82 | 3.47 | 8.0 | 7.11 | 3.47 | 4.1 |

TABLE VI. Comparison between HF results obtained with parameter set (e) (HF) and experimental values (Expt.) for finite nuclei. The nonrelativistic center-of-mass correction is indicated by c.m. (in MeV). Symbols and units are the same as in Table V.

| | $^{16}$O | | | $^{40}$Ca | | | $^{48}$Ca | | | $^{90}$Zr | | $^{208}$Pb | |
|---|---|---|---|---|---|---|---|---|---|---|---|---|---|
| | $-E/A$ | $r_c$ | $\Delta_{LS}$ | $-E/A$ | $r_c$ | $\Delta_{LS}$ | $-E/A$ | $r_c$ | $\Delta_{LS}$ | $-E/A$ | $r_c$ | $-E/A$ | $r_c$ |
| HF | 5.61 | 2.73 | 7.3 | 6.82 | 3.47 | 8.0 | 7.10 | 3.47 | 4.1 | 7.40 | 4.26 | 6.74 | 5.47 |
| Expt. | 7.98 | 2.73 | 6.3 | 8.55 | 3.48 | 7.2 | 8.67 | 3.47 | 4.3 | 8.71 | 4.27 | 7.87 | 5.50 |
| c.m. | 0.61 | | | 0.20 | | | 0.18 | | | 0.08 | | 0.02 | |

where the role of an isovector meson, for $N \neq Z$ nuclei, can be seen. The isovector nature of the pion is crucial to get the correct order of magnitude for the proton spin-orbit splitting and, in particular, to reproduce its drastic change when going from $^{40}$Ca to $^{48}$Ca, although the number of protons is the same in both nuclei.

The $\rho$ meson helps to increase the binding energy. It also plays a role in the spin-orbit splitting, especially the tensor term, since results are quite different when we use either small or strong tensor coupling. The ability to describe correctly spin-orbit splittings over the whole range of mass number is perhaps the major advantage of the present approach over nonrelativistic HF models.

Once the scalar mass is adjusted to get the rms radius of $^{16}$O, all the other radii agree also with experiment within 1% or less. The particular range of the meson-induced interactions is certainly very important in determining the surface properties of finite nuclei.

On the whole, results are obviously better when going from a Hartree to a Hartree-Fock description of finite nuclei including the four mesons. A strong $\rho$-tensor coupling seems also to be preferred by our results, in the sense that our choice $f_\rho/g_\rho = 3.7$ simulates a strong coupling with correlated wave functions (see Sec. III B). In Table VI the results corresponding to the most complete case [set (e)] are compared to the experimental values. Since center-of-mass corrections have not been considered in our calculations, we list also binding energy corrections taken from a nonrelativistic HF calculation[25] as an indicative estimate. Clearly, the calculated nuclei are not enough bound, since about 1.5 MeV are missing over the whole range of nuclei. However, the inclusion of Fock terms gives a very reasonable $A$ dependence of the binding energy, which is not the case in the Hartree approximation. Correlation effects which are beyond the present approach could possibly further increase the calculated binding energies.

The single-particle spectra for both protons and neutrons are given in Table VII. They correspond to the HF approximation with parameter set (e) of Table I. The agreement with experiment is reasonable, although there is some level crossing near the Fermi surface of $^{40}$Ca and $^{48}$Ca. The spectrum for $^{208}$Pb is shown in Fig. 8. The comparison with experiment indicates that the calculated baryon effective mass is too small. In any case, the overly small level density around the Fermi level is a common feature of all HF calculations. In the nonrelativistic approach, many calculations have shown the large effects due to the coupling of HF levels to collective modes of the nucleus and the resulting increase in level density.[26] We can expect similar effects in the relativistic approach, but such a study remains to be done.

The charge density is calculated from the proton density $\rho_{B,\mathrm{p}}$ [Eq. (B5b) of Appendix B]

$$\rho_c(r) = \int d^3r' \rho_{B,\mathrm{p}}(r') g(|\mathbf{r}-\mathbf{r}'|) , \tag{63}$$

where the form factor is taken as a Gaussian:

$$g(r) = (r_0\sqrt{\pi})^{-3} e^{-(r/r_0)^2} ,$$

with $r_0 = \sqrt{2/3}\langle r_\mathrm{p}\rangle_{\mathrm{rms}}$, the rms charge radius of the proton being taken at its free value $\langle r_\mathrm{p}\rangle_{\mathrm{rms}} = 0.8$ fm.

The charge densities corresponding to case (e) of Table I are shown in Fig. 9. The general agreement obtained in

TABLE VII. Single-particle binding energies (in MeV) for protons and neutrons calculated with parameter set (e). Some experimental energies taken from the compilation of Ref. 25 are also shown.

| | $^{16}$O | | | | $^{40}$Ca | | | | $^{48}$Ca | | | |
|---|---|---|---|---|---|---|---|---|---|---|---|---|
| | Protons | | Neutrons | | Protons | | Neutrons | | Protons | | Neutrons | |
| | Calc. | Expt. | Calc. | Expt. | Calc. | Expt. | Calc. | Expt. | Calc. | Expt. | Calc. | Expt. |
| $1s_{1/2}$ | 38.8 | 40±8 | 43.0 | 47 | 48.3 | 50±11 | 56.2 | | 55.0 | 55±9 | 58.3 | |
| $1p_{3/2}$ | 18.3 | 18.4 | 22.3 | 21.8 | 32.5 | | 40.4 | | 39.9 | | 42.1 | |
| | | | | | | 34±6 | | | | 35±7 | | |
| $1p_{1/2}$ | 11.1 | 12.1 | 14.9 | 15.7 | 27.8 | | 35.5 | | 38.0 | | 39.0 | |
| $1d_{5/2}$ | | | | | 16.3 | 15.5 | 23.9 | 21.9 | 23.3 | 20 | 25.1 | 16 |
| $2s_{1/2}$ | | | | | 7.7 | 10.9 | 15.1 | 18.2 | 14.0 | 15.8 | 16.8 | 12.4 |
| $1d_{3/2}$ | | | | | 8.3 | 8.3 | 15.6 | 15.6 | 19.3 | 15.3 | 19.6 | 12.4 |
| $1f_{7/2}$ | | | | | | | | | | | 9.0 | 9.9 |

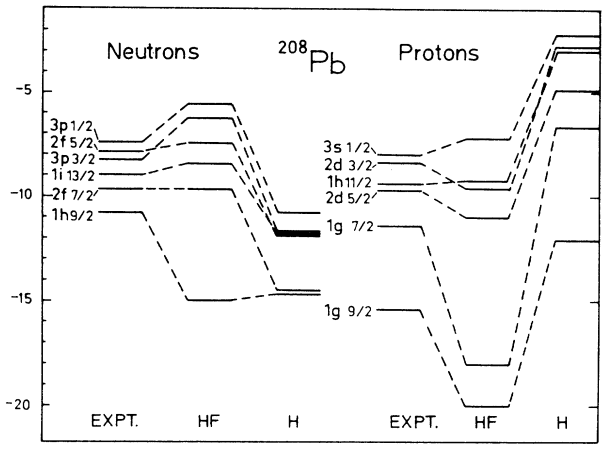


FIG. 8. Calculated and experimental single-particle energies (in MeV) in $^{208}$Pb. The calculations are done with parameter sets (a) ($H$, Hartree approximation) and (e) (HF, Hartree-Fock approximation).

our model is comparable to the most realistic nonrelativistic calculations. The description of the nuclear surface is rather good, in any case better than in the Hartree approximation. This is probably due to the smaller value of the incompressibility parameter in nuclear matter, and also to a large value of the surface contribution to this parameter.

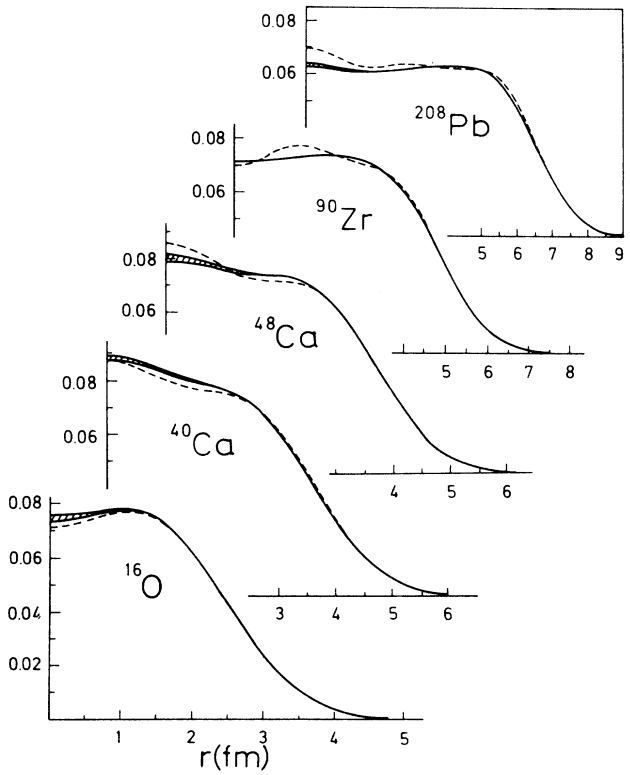


FIG. 9. Calculated (dashed lines) and experimental (Ref. 27) (solid lines) charge distributions in $^{16}$O, $^{40}$Ca, $^{48}$Ca, $^{90}$Zr, and $^{208}$Pb. The shaded areas correspond to experimental uncertainties.

### C. Momentum distribution in nuclei

It is interesting to compare the momentum distribution in nuclei in a nonrelativistic calculation (with Skyrme interaction) and the relativistic model described in this work. We start with the Fourier transform of the baryon spinor $f_\alpha(\mathbf{r})$,

$$\tilde{f}_\alpha(\mathbf{k})=\frac{1}{(2\pi)^{3/2}}\int d^3r\, e^{i\mathbf{k}\cdot\mathbf{r}} f_\alpha(\mathbf{r})\ , \tag{64}$$

which can be decomposed as

$$\tilde{f}_\alpha(\mathbf{k})=\begin{bmatrix} i\tilde{G}_a(k) \\ \tilde{F}_a(k)\boldsymbol{\sigma}\cdot\hat{\mathbf{k}} \end{bmatrix} \mathcal{Y}_\alpha(\hat{\mathbf{k}})\chi_{1/2}(q_a) \tag{65}$$

The momentum distribution for spherical nuclei is then written as

$$n(k)=\frac{1}{4\pi}\sum_a \hat{j}_a^2[\,|\,\tilde{G}_a(k)\,|^2+|\,\tilde{F}_a(k)\,|^2]\ , \tag{66}$$

and is normalized to the total number of particles:

$$\int d^3k\, n(k)=A\ . \tag{67}$$

It turns out that in the two calculations (relativistic and nonrelativistic) the momentum distribution is practically the same in a reasonable range of momentum (0—400 MeV) once the rms radius of the nucleus is adjusted to the same value in both calculations. This somehow surprising result may be another confirmation that the Skyrme energy functional incorporates most of the relativistic features that are exhibited in our microscopic derivation and which have already been discussed in Secs. III D and III E.

### D. Magnetic moments of odd nuclei

There has been a lot of concern about relativistic corrections to magnetic moments of nuclei with one particle (proton) or hole on top of a closed shell, for instance, $^{15}$N and $^{17}$F, and also $^{39}$K and $^{41}$Sc. It appears[28] that in the mean field approximation corrections to the Schmidt value of the orbital magnetic moment (Dirac moment) are of the order of 100% for $^{15}$N ($j=l-\frac{1}{2}$) and only 15% for $^{17}$F ($j=l+\frac{1}{2}$). These corrections are mainly attributed to the effective mass, although particular cancellations arise for nuclei in which the active single-particle state corresponds to $j=1+\frac{1}{2}$. However, the Dirac moment is rather sensitive to the value of the $\Sigma_V$ self-energy which appears, for instance, if Fock terms are included, or if core polarization effects, due to the spatial component of $\omega$ exchange, are taken into account. We obtain in the present HF calculations nearly the same Dirac magnetic moments as in the simple Hartree case, once the different coupling constants are renormalized. It has been pointed out[29] that, in order to conserve the electromagnetic current (gauge invariance), corrections to the operator itself should be taken into account in addition to wave function corrections. This can be done according to the vector Ward identity (in nuclear matter, for instance):

$$(p'-p)_\mu \Lambda^\mu(p,p') = -\frac{1+\tau_3}{2}[\Sigma(p')-\Sigma(p)] , \quad (68)$$

where $p$ and $p'$ are the initial and final momenta of the nucleon, and $\Lambda^\mu$ is the correction to the free electromagnetic operator $\gamma^\mu$. Such an equation gives no corrections in the mean field approximation (the self-energies are independent of the momentum for an inert, closed core). In the HF approximation, some vertex corrections are expected. More importantly, random phase approximation— (RPA-) type correlations will modify the self-energies and may give the dominant vertex renormalizations. In nuclear matter, the importance of these long range correlations for isoscalar transitions has been shown.[30] In finite nuclei such calculations have not yet been done.

### E. Connection with nonrelativistic Hartree-Fock models

It is already known[31–33] that the Skyrme Hartree-Fock Hamiltonian can be recovered from a $1/M$ expansion of the relativistic equation, at least in the Hartree approximation. Again, this correspondence can be seen as another interpretation of the Skyrme interaction.

More precisely, the HF approximation with nonrelativistic effective interactions is very successful in describing nuclear binding energies and charge distributions.[34] This success has been achieved after it was realized that a density dependence of the effective interaction was needed and that such a density dependence, at least qualitatively, stems from the properties of the $G$ matrix. Since a relativistic HF description also seems to be satisfactory for binding energies and charge densities, it is worthwhile to examine how the binding energy comes about in a relativistic and a nonrelativistic approach.

In the relativistic case, with the Hamiltonian used in this work, the binding energy obeys Eq. (61), which we rewrite as

$$E^R/A = \tfrac{1}{2}\sum_{\alpha=1}^{A} t_\alpha^R/A + \tfrac{1}{2}\sum_{\alpha=1}^{A} \epsilon_\alpha^R/A \equiv t^R + \epsilon^R . \quad (69)$$

The nonrelativistic HF energy per particle is

$$E^{\rm NR}/A = \tfrac{1}{2}\sum_{\alpha=1}^{A} t_\alpha^{\rm NR}/A + \tfrac{1}{2}\sum_{\alpha=1}^{A} \epsilon_\alpha^{\rm NR}/A + E_r$$
$$\equiv t^{\rm NR} + \epsilon^{\rm NR} + E_r , \quad (70)$$

where $t_\alpha^{\rm NR}$ is calculated with the operator $-\nabla^2/2M$, and $E_r$ is the rearrangement energy per particle coming from the density dependence of the effective interaction.

First, one can show[35] that $t^R$ is smaller than $t^{\rm NR}$ if the nonrelativistic wave functions are well approximated by the upper components $G_\alpha$ of the relativistic ones, i.e., the conclusions concerning the kinetic energy in nuclear matter can be extended qualitatively to finite nuclei. To make the argument simple, we just consider the $(\sigma,\omega)$ mean field model, where we have only scalar and timelike vector potentials, $\Sigma_S(r)$ and $\Sigma_0(r)$. The quantity $t^R$ can be expressed in terms of the lower components $F_\alpha$ as

TABLE VIII. Components of the binding energy per particle for the nucleus $^{40}$Ca, calculated with Skyrme force SIII and parameter set (e). All quantities are in MeV.

| | NR (SIII) | $R$ [case (e)] |
|---|---|---|
| $t$ | 8.2 | 5.8 |
| $\epsilon$ | −10.9 | −12.6 |
| $E_r$ | −5.6 | 0 |
| $E/A$ | −8.3 | −6.8 |

$$t^R = \sum_{\alpha=1}^{A} \int F_\alpha^2(r)[E_\alpha + \Sigma_S(r) - \Sigma_0(r)]dr . \quad (71)$$

On the other hand, if one calculates $t^{\rm NR}$ using the $G_\alpha$ as wave functions (i.e., up to corrections of order $F_\alpha^2/G_\alpha^2$ due to normalization) and expresses the result in terms of $F_\alpha$ by means of the Hartree-Dirac equation, one finds

$$t^{\rm NR} = \frac{1}{4M}\sum_{\alpha=1}^{A} \int F_\alpha^2(r)[E_\alpha + M + \Sigma_S(r) - \Sigma_0(r)]^2 dr . \quad (72)$$

Thus, the quantity

$$t^R - t^{\rm NR} = -\frac{1}{4M}\sum_{\alpha=1}^{A} \int F_\alpha^2(r)[E_\alpha - M + \Sigma_S(r) - \Sigma_0(r)]^2 dr \quad (73)$$

is always negative.

From this result, one can see that if the two models are to give approximately the same binding energies and densities, then $\epsilon^{\rm NR}$ has to be more negative than $\epsilon^R$ and/or $E_r$ must give a negative contribution. As an illustration, we compare in Table VIII the components of the binding energy per particle in the nucleus $^{40}$Ca for two realistic cases. The relativistic HF model is that of parameter set (e) of Table I, while the nonrelativistic model is calculated with the standard SIII Skyrme interaction[34] without center-of-mass correction to make the comparison clear. Although $E^R/A$ is larger than $E^{\rm NR}/A$, both $t^R$ and $\epsilon^R$ are, respectively, below $t^{\rm NR}$ and $\epsilon^{\rm NR}$. If we had forced a fit to impose $E^R/A \simeq -8.3$ MeV in $^{40}$Ca, for instance, by allowing $f_\rho$ to be slightly larger, $t^R$ and $\epsilon^R$ would be even lower.

## V. FINAL REMARKS

We have presented a consistent microscopic description of two complementary aspects of nuclear structure, namely infinite nuclear matter and ground state properties of closed shell nuclei covering a large range of mass number. In the framework of relativistic quantum field theory, which incorporates very naturally the meson degrees of freedom underlying the NN potential, we applied a relativistic HF approximation restricted to tree level contributions. We have particularly emphasized the contributions coming from the exchange (Fock) part of the interaction and the contributions of the isovector mesons ($\pi$ and $\rho$).

In this context, it appears that a complete information about the validity of this relativistic microscopic description can only be achieved by looking at both infinite nu-

clear matter and finite nuclei. In particular, all the surface properties which fix to a large extent the overall properties of finite nuclei are governed by the finite range of the interactions. It turns out that a reasonable agreement can be obtained with the experimental properties of nuclear ground states. The spin-orbit splittings over the whole range of mass numbers come out very naturally. In the present HF approximation, the underlying NN potential is in qualitative agreement with the free potential, the medium corrections being contained in the renormalization of the isoscalar coupling constants.

The relationship with traditional nonrelativistic approaches can be achieved by looking at the low-momentum limit of our relativistic formalism. Two different corrections can be exhibited: On one hand, relativistic kinematical corrections are not negligible, and reflect the fact that the mean value of the nucleon velocity in the medium is about $(0.35-0.40)c$ at normal nuclear density, with the interactions derived from the free NN potential. These kinematical corrections in infinite matter amount to about 10 MeV of repulsion at normal nuclear density. On the other hand, nontrivial corrections coming from the presence of negative energy components in the relativistic nucleon wave function inside the medium generate a new density dependence in the energy functional and account for the shift of the saturation point in nuclear matter towards smaller density, together with a repulsion of about 8 MeV. We pointed out, however, that such contributions have already been introduced, at the phenomenological level, in the construction of effective interactions of the Skyrme type, for instance. With such a density dependence, it appears that the saturation of nuclear matter, with a relativistic NN interaction, is already achieved in the HF approximation, contrary to most of the nonrelativistic descriptions.

The understanding, at a microscopic level, of such an energy functional is essential in the present development of intermediate energy physics. In particular, the quantitative description of finite nuclei is certainly an important step in the modeling of nuclear physics in terms of nucleon and meson degrees of freedom. Corrections to the present scheme can be made in two different directions. On one hand, nuclear correlations have certainly to be incorporated, in both nuclear matter *and* finite nuclei. This has partly been done already in nuclear matter for short range (Brueckner type) and also long range (RPA type) correlations. One may include also, in that part, contributions coming from three- and many-body forces. These can be generated either from excitations of nuclear resonances (isobar, for instance) or from nonlinear couplings of the $\sigma$ field, starting from a more general, chirally symmetric Lagrangian.[36] Such a program has, however, not been fully completed from a quantitative point of view for finite nuclei.

On the other hand, one may think of extending such models to get a closer connection with what one believes is the underlying theory describing nucleon and meson degrees of freedom, namely QCD. The necessity of this connection is obvious at high baryon density (may be 5 times normal nuclear density), where the nucleons are largely overlapping. In that spirit, one should, however, start from a different Lagrangian, in order to be able to incorporate the new degrees of freedom and to take into account the complete structure of the vacuum. This direction is certainly a new way of looking at nuclear physics, not in the sense of invalidating all the "traditional" description of nuclear structure, but of a deeper understanding of the nuclear dynamics.

## ACKNOWLEDGMENTS

One of us (S.M.) is grateful for the hospitality of the Division de Physique Théorique at Orsay. We would like to thank B. Desplanques and J. Treiner for useful discussions.

## APPENDIX A: ENERGY DENSITY AND SELF-ENERGIES IN SYMMETRIC NUCLEAR MATTER

The energy density $\epsilon$ of Eq. (37) can be calculated using the Hamiltonian (18) and the spinors $u(\mathbf{p},s)$ of Eq. (34) describing particle states in the nuclear medium. These spinors are formally identical to free particle spinors $u^{(0)}(\mathbf{p},s)$, the only difference being the replacement of the free quantities $(\mathbf{p},E,M)$ by the starred ones defined in Eq. (31). The calculation of $\epsilon$ therefore requires only standard trace techniques and the repeated use of the projection operator onto positive energy states,

$$\Lambda_+^* = \frac{\not{p}^* + M^*}{2M^*} \ . \tag{A1}$$

For the kinetic energy contribution, one gets

$$\langle T \rangle = \frac{2}{\pi^2} \int_0^{p_F} p^2 dp (p\hat{P} + M\hat{M}) \ , \tag{A2}$$

where $\hat{P}$ and $\hat{M}$ are defined in Eq. (33).

The potential energy $\langle V \rangle$ can be separated into its direct part $\langle V_D \rangle$ [Hartree contributions of Fig. 2(a)] and exchange part $\langle V_E \rangle$ [Fock contributions of Fig. 2(b)]. In symmetric $N=Z$ nuclear matter, isovector mesons do not contribute to the direct potential energy. We therefore have the simple result

$$\langle V_D \rangle = -\frac{1}{2}\left[\frac{g_\sigma}{m_\sigma}\right]^2 \rho_S^2 + \frac{1}{2}\left[\frac{g_\omega}{m_\omega}\right]^2 \rho_B^2 \ , \tag{A3}$$

where $\rho_S$ and $\rho_B$ are, respectively, the scalar and baryonic densities defined as

$$\begin{aligned} \rho_S &= \frac{2}{\pi^2} \int_0^{p_F} p^2 dp \, \hat{M}(p) \ , \\ \rho_B &= \frac{2}{3\pi^2} p_F^3 \ . \end{aligned} \tag{A4}$$

The exchange potential energy is a sum of contributions from all mesons. It can be expressed as

TABLE IX. The functions $A_i$, $B_i$, $C_i$, and $D$ of Eq. (A5).

| $i$ | $A_i$ | $B_i$ | $C_i$ |
|---|---|---|---|
| $\sigma$ | $g_\sigma^2\theta_\sigma$ | $g_\sigma^2\theta_\sigma$ | $-2g_\sigma^2\phi_\sigma$ |
| $\omega$ | $2g_\omega^2\theta_\omega$ | $-4g_\omega^2\theta_\omega$ | $-4g_\omega^2\phi_\omega$ |
| $\rho_V$ | $6g_\rho^2\theta_\rho$ | $-12g_\rho^2\theta_\rho$ | $-12g_\rho^2\phi_\rho$ |
| $\pi_{\rm ps}$ | $3g_\pi^2\theta_\pi$ | $-3g_\pi^2\theta_\pi$ | $-6g_\pi^2\phi_\pi$ |
| $\pi_{\rm pv}$ | $-3\left[\frac{f_\pi}{m_\pi}\right]^2 m_\pi^2\theta_\pi$ | $-3\left[\frac{f_\pi}{m_\pi}\right]^2 m_\pi^2\theta_\pi$ | $6\left[\frac{f_\pi}{m_\pi}\right]^2[(p^2+p'^2)\phi_\pi-pp'\theta_\pi]$ |
| $\rho_T$ | $-3\left[\frac{f_\rho}{2M}\right]^2 m_\rho^2\theta_\rho$ | $-9\left[\frac{f_\rho}{2M}\right]^2 m_\rho^2\theta_\rho$ | $12\left[\frac{f_\rho}{2M}\right]^2[(p^2+p'^2-m_\rho^2/2)\phi_\rho-pp'\theta_\rho]$ |
| $\rho_{VT}$ | $D=36\frac{f_\rho g_\rho}{2M}(p\theta_\rho-2p'\phi_\rho)$ | | |

$$\langle V_E\rangle=\frac{1}{(2\pi)^4}\int_0^{p_F}p\,dp\,p'dp'\left[\sum_i A_i(p,p')+\hat{M}(p)\hat{M}(p')\sum_i B_i(p,p')+\hat{P}(p)\hat{P}(p')\sum_i C_i(p,p')+\hat{P}(p)\hat{M}(p')D(p,p')\right], \tag{A5}$$

where the sums over $i$ include the various cases listed in Table IX. The $D$ term of Eq. (A5) corresponds to the cross vector-tensor $\rho$-N coupling. The expressions for the quantities $A,B,C,D$ are given in Table IX, in terms of the functions

$$\theta_i(p,p')=\ln\left[\frac{m_i^2+(p+p')^2}{m_i^2+(p-p')^2}\right],$$
$$\phi_i(p,p')=\frac{p^2+p'^2+m_i^2}{4pp'}\theta_i(p,p')-1. \tag{A6}$$

These expressions include the removal of the zero-range interactions in the pseudovector-pion and tensor-$\rho$ contributions as discussed in Sec. II E. The pseudoscalar-pion case is also listed in Table IX, although it is not used in this work.

The self-energies (29) are obtained by differentiating $\langle V\rangle$ with respect to $u(\mathbf{p},s)$. This can easily be done by using the relations

$$\hat{M}(p)=\tfrac{1}{2}\sum_s\bar{u}(\mathbf{p},s)u(\mathbf{p},s),$$
$$\hat{P}(p)=\tfrac{1}{2}\sum_s\bar{u}(\mathbf{p},s)\boldsymbol{\gamma}\cdot\hat{\mathbf{p}}\,u(\mathbf{p},s), \tag{A7}$$
$$1=\tfrac{1}{2}\sum_s\bar{u}(\mathbf{p},s)\gamma_0 u(\mathbf{p},s).$$

We thus get

$$\Sigma_S(p)=-\left[\frac{g_\sigma}{m_\sigma}\right]^2\rho_S+\frac{1}{(4\pi)^2}\frac{1}{p}\int_0^{p_F}p'dp'\left[\hat{M}(p')\sum_i B_i(p,p')+\tfrac{1}{2}\hat{P}(p')D(p',p)\right],$$
$$\Sigma_0(p)=\left[\frac{g_\omega}{m_\omega}\right]^2\rho_B+\frac{1}{(4\pi)^2}\frac{1}{p}\int_0^{p_F}p'dp'\sum_i A_i(p,p'), \tag{A8}$$
$$\Sigma_V(p)=\frac{1}{(4\pi)^2}\frac{1}{p}\int_0^{p_F}p'dp'\left[\hat{P}(p')\sum_i C_i(p,p')+\tfrac{1}{2}\hat{M}(p')D(p,p')\right].$$

## APPENDIX B: HARTREE FOCK EQUATIONS FOR SPHERICAL NUCLEI

We give here the detailed expressions of the quantities entering the HF equations (60). The notations are those of Sec. IV. We also introduce the notation $\alpha'=(q_a,n_a,l'_a,j_a,m_a)=(a',m_a)$, where

$$l'_a=\begin{cases}l_a+1 & \text{if } j_a=l_a+\frac{1}{2},\\ l_a-1 & \text{if } j_a=l_a-\frac{1}{2}.\end{cases} \tag{B1}$$

In the following, we often need the reduced matrix elements of the tensorial operators $Y_L^m(\hat{\mathbf{r}})$ and

$$T^M_{\mathscr{J}L} \equiv \sum_{mk} (L\ 1\ m\ k\ |\ \mathscr{J}M) Y_L^m(\hat{\mathbf{r}}) \sigma^k \ . \tag{B2}$$

They are given as

$$\langle a||Y_L||b\rangle = \begin{cases} (4\pi)^{-1/2} \hat{j}_a \hat{j}_b \hat{L} (-1)^{j_b - L - 1/2} \begin{pmatrix} j_a & j_b & L \\ \frac{1}{2} & -\frac{1}{2} & 0 \end{pmatrix} & \text{if } l_a + l_b + L \text{ is even} \ , \\ 0 \ \text{ if } l_a + l_b + L \text{ is odd} \ , \end{cases} \tag{B3}$$

$$\langle a||T_{\mathscr{J}L}||b\rangle = \left( \frac{6}{4\pi} \right)^{1/2} (-1)^{l_a} \hat{j}_a \hat{j}_b \hat{l}_a \hat{l}_b \hat{\mathscr{J}} \hat{L} \begin{pmatrix} l_a & L & l_b \\ 0 & 0 & 0 \end{pmatrix} \begin{Bmatrix} j_a & j_b & \mathscr{J} \\ l_a & l_b & L \\ \frac{1}{2} & \frac{1}{2} & 1 \end{Bmatrix} , \tag{B4}$$

where $\hat{J} = \sqrt{2J+1}$.

The radial parts of the neutron and proton scalar ($S$), baryonic ($B$), and tensor ($T$) densities are

$$\rho_{S,\ \mathrm{n\ or\ p}} = \frac{1}{4\pi r^2} \sum_{b\ (\mathrm{n\ or\ p})} \hat{j}_b^2 [G_b^2(r) - F_b^2(r)] \ , \tag{B5a}$$

$$\rho_{B,\ \mathrm{n\ or\ p}} = \frac{1}{4\pi r^2} \sum_{b\ (\mathrm{n\ or\ p})} \hat{j}_b^2 [G_b^2(r) + F_b^2(r)] \ , \tag{B5b}$$

$$\rho_{T,\ \mathrm{n\ or\ p}} = \frac{1}{4\pi r^2} \sum_{b\ (\mathrm{n\ or\ p})} \hat{j}_b^2 [2G_b(r) F_b(r)] \ . \tag{B5c}$$

The sums over $b$ run over occupied orbitals, and the subscripts n,p stand for neutrons and protons, respectively. The total densities are given by

$$\begin{aligned} \rho_S &= \rho_{S,\mathrm{n}} + \rho_{S,\mathrm{p}} \ , \\ \rho_B &= \rho_{B,\mathrm{n}} + \rho_{B,\mathrm{p}} \ , \\ \rho_T &= \rho_{T,\mathrm{n}} + \rho_{T,\mathrm{p}} \ . \end{aligned} \tag{B6}$$

The expressions of the direct and exchange terms entering the HF equations (60) are obtained in coordinate space by using multipole expansions of the meson propagators:

$$\frac{e^{-m|\mathbf{r}_1 - \mathbf{r}_2|}}{|\mathbf{r}_1 - \mathbf{r}_2|} = 4\pi m \sum_L \tilde{I}_L(z_<) \tilde{K}_L(z_>) Y_L(\hat{\mathbf{r}}_1) \cdot Y_L(\hat{\mathbf{r}}_2) \ , \tag{B7}$$

where $z_<$ ($z_>$) denotes the smaller (larger) of $z_1$ and $z_2$, with $z_i = m r_i$. We have introduced the notation

$$\begin{pmatrix} \tilde{I}_L(z) \\ \tilde{K}_L(z) \end{pmatrix} = \frac{1}{\sqrt{z}} \begin{pmatrix} I_{L+1/2}(z) \\ K_{L+1/2}(z) \end{pmatrix} , \tag{B8}$$

where $I$ and $K$ are the modified spherical Bessel functions of the first and third kind.

### 1. Direct terms

The pion does not contribute to the direct terms. The Hartree contributions $\Sigma_S^D$, $\Sigma_0^D$, and $\Sigma_T^D$ to the self-energies in Eq. (60) are

$$\Sigma^D_{T,a}(r) = [V_T(r) + V^{(1)}_{VT}(r)] q_a \ , \tag{B9a}$$

$$\Sigma^D_{S,a}(r) = V_\sigma(r) \ , \tag{B9b}$$

$$\Sigma^D_{0,a}(r) = V_\omega(r) + [V_\rho(r) + V^{(2)}_{VT}(r)] q_a + \tfrac{1}{2}(1 + q_a) V_c(r) \ . \tag{B9c}$$

The various terms evidently correspond to the contributions from $\sigma$, $\omega$, and $\rho$ mesons (the latter is decomposed into vector, tensor, and cross vector-tensor terms) and the Coulomb potential. Their explicit expressions are

$$\begin{aligned} V_c(r) &= e^2 \int_0^\infty \frac{\rho_{B,\mathrm{p}}(r')}{r_>} r'^2 dr' \ , \\ V_\sigma(r) &= -g_\sigma^2 m_\sigma \int_0^\infty \rho_S(r') \tilde{I}_0(z_<) \tilde{K}_0(z_>) r'^2 dr' \ , \\ V_\rho(r) &= g_\rho^2 m_\rho \int_0^\infty [\rho_{B,\mathrm{p}}(r') - \rho_{B,\mathrm{n}}(r')] \tilde{I}_0(z_<) \tilde{K}_0(z_>) r'^2 dr' \ , \end{aligned} \tag{B10}$$

while $V_\omega(r)$ is similar to $V_\sigma(r)$ with $(-g_\sigma^2, m_\sigma)$ and $\rho_S$ replaced by $(g_\omega^2, m_\omega)$ and $\rho_B$, respectively. The other contributions from the $\rho$ meson are

$$\begin{aligned} V^{(1)}_{VT}(r) &= \frac{-f_\rho}{2M g_\rho} \frac{d}{dr} V_\rho(r) \ , \\ V^{(2)}_{VT}(r) &= -\left[ \frac{g_\rho f_\rho}{2M} \right] m_\rho \int_0^\infty [\rho_{T,\mathrm{p}}(r') - \rho_{T,\mathrm{n}}(r')] \\ &\quad \times \left[ \frac{d}{dr'} \tilde{I}_0(z_<) \tilde{K}_0(z_>) \right] r'^2 dr' , \end{aligned} \tag{B11}$$

$$\begin{aligned} V_T(r) = -\left[ \frac{f_\rho}{2M} \right]^2 \Big\{ & m_\rho^3 \int_0^\infty [\rho_{T,\mathrm{p}}(r') - \rho_{T,\mathrm{n}}(r')] \\ & \times \tilde{I}_1(z_<) \tilde{K}_1(z_>) r'^2 dr' \\ & - (1 - \tfrac{1}{3}) [\rho_{T,\mathrm{p}}(r) - \rho_{T,\mathrm{n}}(r)] \Big\} . \end{aligned}$$

The term $\frac{1}{3}(\rho_{T,\mathrm{p}} - \rho_{T,\mathrm{n}})$ in $V_T(r)$ arises from the removal of the $\delta(\mathbf{r}_1 - \mathbf{r}_2)$ part in the $\rho$-induced interaction.

### 2. Exchange terms

The quantities $X$ and $Y$ of Eq. (60) are obtained by summing the contributions of the various mesons (we omit the obvious subscript $a$).

*(a) $\sigma$ meson.* We have

$$X^{(\sigma)}(r)=-g_\sigma^2 m_\sigma \hat{j}_a^{-2}\sum_b \delta_{q_a,q_b}F_b(r)\sum_L |\langle a||Y_L||b\rangle|^2\int_0^\infty [G_aG_b-F_aF_b]_{r'}\tilde{I}_L(z_<)\tilde{K}_L(z_>)dr' , \tag{B12}$$

the sum over $b$ running over occupied states. The expression for $Y^{(\sigma)}$ is similar, with an opposite overall sign and $F_b(r)$ replaced by $G_b(r)$.

*(b) $\omega$ meson.* The time component of the $\omega$ coupling gives

$$X^{(\omega_0)}(r)=-g_\omega^2 m_\omega \hat{j}_a^{-2}\sum_b \delta_{q_a,q_b}F_b(r)\sum_L |\langle a||Y_L||b\rangle|^2\int_0^\infty [G_aG_b+F_aF_b]_{r'}\tilde{I}_L(z_<)\tilde{K}_L(z_>)dr' , \tag{B13}$$

while $Y^{(\omega_0)}$ has a similar expression with the first $F_b(r)$ replaced by $G_b(r)$.

From the space component we obtain

$$X^{(\omega)}(r)=-g_\omega^2 m_\omega \hat{j}_a^{-2}\sum_b \delta_{q_a,q_b}G_b(r)\sum_{Lf}\langle a'||T_{fL}||b\rangle\int_0^\infty [\langle a||T_{fL}||b'\rangle F_aG_b-\langle a'||T_{fL}||b\rangle G_aF_b]_{r'}\tilde{I}_L(z_<)\tilde{K}_L(z_>)dr' , \tag{B14a}$$

$$Y^{(\omega)}(r)=-g_\omega^2 m_\omega \hat{j}_a^{-2}\sum_b \delta_{q_a,q_b}F_b(r)\sum_{Lf}\langle b'||T_{fL}||a\rangle\int_0^\infty [\langle b||T_{fL}||a'\rangle G_aF_b-\langle b'||T_{fL}||a\rangle F_aG_b]_{r'}\tilde{I}_L(z_<)\tilde{K}_L(z_>)dr' . \tag{B14b}$$

*(c) $\pi$ meson.* With the pion pseudovector coupling one has

$$X^{(\pi)}(r)=f_\pi^2\hat{j}_a^{-2}\sum_b(2-\delta_{q_a,q_b})F_b(r)\left\{\frac{\hat{j}_a^2\hat{j}_b^2}{8\pi}\frac{[G_aG_b+F_aF_b]_r}{m_\pi^2 r^2}\right.$$
$$+m_\pi\sum_L\hat{L}^{-4}|\langle a||Y_L||b'\rangle|^2\sum_{L_1L_2}[\kappa_{ab}-\alpha(L_1)]i^{L_2-L_1}$$
$$\left.\times\int_0^\infty[(\kappa_{ab}+\alpha(L_2))G_aG_b-(\kappa_{ab}-\alpha(L_2))F_aF_b]_{r'}R_{L_1L_2}(r,r')dr'\right\} , \tag{B15}$$

where

$$\alpha(L_1)=\begin{cases}-L & \text{if } L_1=L-1\\ L+1 & \text{if } L_1=L+1\end{cases} ,$$

and $\kappa_{ab}=\kappa_a+\kappa_b$. Here and in the following, $L_1$ and $L_2$ can only take the values $L\pm1$, and

$$R_{L_1L_2}(r,r')\equiv\tilde{I}_{L_1}(z)\tilde{K}_{L_2}(z')\theta(z'-z)+\tilde{K}_{L_1}(z)\tilde{I}_{L_2}(z')\theta(z-z') . \tag{B16}$$

The expression for $Y^{(\pi)}(r)$ is obtained from Eq. (B15) by interchanging all $F$ and $G$ and replacing $\kappa_{ab}$ by $-\kappa_{ab}$. The $\delta(\mathbf{r}_1-\mathbf{r}_2)$ piece which arises in pseudovector coupling can be removed by adding

$$\delta X^{(\pi)}(r)=\frac{-f_\pi^2\hat{j}_a^{-2}}{3}\sum_b(2-\delta_{q_a,q_b})\frac{F_b(r)}{m_\pi^2r^2}\sum_{Lf}\langle a'||T_{fL}||b'\rangle[\langle a||T_{fL}||b\rangle G_aG_b+\langle a'||T_{fL}||b'\rangle F_aF_b]_r ,$$
$$\delta Y^{(\pi)}(r)=\frac{-f_\pi^2\hat{j}_a^{-2}}{3}\sum_b(2-\delta_{q_a,q_b})\frac{G_b(r)}{m_\pi^2r^2}\sum_{Lf}\langle a||T_{fL}||b\rangle[\langle a||T_{fL}||b\rangle G_aG_b+\langle a'||T_{fL}||b'\rangle F_aF_b]_r . \tag{B17}$$

For completeness, we also give the expression corresponding to the case of pseudoscalar coupling:

$$X^{(\pi)}(r)=g_\pi^2 m_\pi \hat{j}_a^{-2}\sum_b(2-\delta_{q_a,q_b})G_b(r)\sum_L\langle a||Y_L||b'\rangle\langle a'||Y_L||b\rangle\int_0^\infty[G_aF_b+F_aG_b]_{r'}\tilde{I}_L(z_<)\tilde{K}_L(z_>)dr' , \tag{B18}$$

while $Y^{(\pi)}(r)$ is deduced by interchanging all $F$ and $G$.

*(d) $\rho$ meson.* The vector part of the $\rho$ meson gives $X(r)$ and $Y(r)$ which are formally identical to those of the $\omega$ meson, except for the isospin factor $\delta_{q_a,q_b}$, which is replaced by $2-\delta_{q_a,q_b}$.

The tensor term in the starting Lagrangian gives rise to two types of contributions. They are proportional to $f_\rho^2$ and $f_\rho g_\rho$, and they are denoted, respectively, by $(X^{(T)},Y^{(T)})$ and $(X^{(VT)},Y^{(VT)})$. Furthermore, it is convenient to separate in the tensor coupling $\sigma^{\mu k}q_k$ contributions coming either from $\mu=0$ or from $\mu=(1,2,3)$. They are referred to by the superscripts 1 and 2.

For $X^{(T)}$ and $Y^{(T)}$ we have

$$X^{(T,1)}(r)=-\left[\frac{f_\rho}{2M}\right]^2 m_\rho^2\hat{j}_a^{-2}\sum_b(2-\delta_{q_a,q_b})G_b(r)$$
$$\times\left\{\frac{\hat{j}_a^2\hat{j}_b^2}{8\pi}\frac{[G_aF_b+F_aG_b]_r}{m_\rho^2r^2}+m_\rho\sum_L\hat{L}^{-4}|\langle a||Y_L||b\rangle|^2\sum_{L_1L_2}i^{L_2-L_1}(\tilde{\kappa}_{ab}-\alpha(L_1))\right.$$
$$\left.\times\int_0^\infty[(\tilde{\kappa}_{ab}+\alpha(L_2))G_aF_b-(\tilde{\kappa}_{ab}-\alpha(L_2))F_aG_b]_{r'}R_{L_1L_2}(r,r')dr'\right\}, \tag{B19}$$

where $\tilde{\kappa}_{ab}=\kappa_a-\kappa_b$. The quantity $Y^{(T,1)}$ can be obtained by interchanging all $F$ and $G$ and replacing $\tilde{\kappa}_{ab}$ by $-\tilde{\kappa}_{ab}$. The $X^{(T,2)}$ term is

$$X^{(T,2)}(r)=6\left[\frac{f_\rho}{2M}\right]^2 m_\rho^2\hat{j}_a^{-2}\sum_b(2-\delta_{q_a,q_b})F_b(r)$$
$$\times\sum_{L\mathcal{J}}\sum_{L_1L_2}f_{L\mathcal{J}}(L_1)f_{L\mathcal{J}}(L_2)\langle a'||T_{\mathcal{J}L_1}||b'\rangle\int_0^\infty[\langle a||T_{\mathcal{J}L_2}||b\rangle G_aG_b-\langle a'||T_{\mathcal{J}L_2}||b'\rangle F_aF_b]_{r'}$$
$$\times[m_\rho R_{L_1L_2}(r,r')-\delta(r-r')]dr', \tag{B20}$$

where we have introduced

$$f_{L\mathcal{J}}(L_1)\equiv\hat{L}\hat{L}_1\begin{bmatrix}L_1 & L & 1\\ 0 & 0 & 0\end{bmatrix}\begin{Bmatrix}L_1 & L & 1\\ 1 & 1 & \mathcal{J}\end{Bmatrix}.$$

The corresponding $Y^{(T,2)}$ is obtained by replacing the first $F_b(r)$ by $G_b(r)$, $\langle a'||T_{\mathcal{J}L_1}||b'\rangle$ by $\langle a||T_{\mathcal{J}L_1}||b\rangle$, and changing the overall sign. To remove the contributions of the $\delta(\mathbf{r}_1-\mathbf{r}_2)$ term, one has to add

$$\delta X^{(T,1)}(r)=\frac{1}{3}\left[\frac{f_\rho}{2M}\right]^2\hat{j}_a^{-2}\sum_b(2-\delta_{q_a,q_b})\frac{G_b(r)}{r^2}\sum_{\mathcal{J}L}\langle a'||T_{\mathcal{J}L}||b\rangle[\langle a||T_{\mathcal{J}L}||b'\rangle G_aF_b+\langle a'||T_{\mathcal{J}L}||b\rangle F_aG_b]_r,$$
$$\delta Y^{(T,1)}(r)=\frac{1}{3}\left[\frac{f_\rho}{2M}\right]^2\hat{j}_a^{-2}\sum_b(2-\delta_{q_a,q_b})\frac{F_b(r)}{r^2}\sum_{\mathcal{J}L}\langle a||T_{\mathcal{J}L}||b'\rangle[\langle a||T_{\mathcal{J}L}||b'\rangle G_aF_b+\langle a'||T_{\mathcal{J}L}||b\rangle F_aG_b]_r, \tag{B21}$$

$$\delta X^{(T,2)}(r)=\frac{2}{3}\left[\frac{f_\rho}{2M}\right]^2\hat{j}_a^{-2}\sum_b(2-\delta_{q_a,q_b})\frac{F_b(r)}{r^2}\sum_{\mathcal{J}L}\langle a'||T_{\mathcal{J}L}||b'\rangle[\langle a||T_{\mathcal{J}L}||b\rangle G_aG_b-\langle a'||T_{\mathcal{J}L}||b'\rangle F_aF_b]_r,$$
$$\delta Y^{(T,2)}(r)=-\frac{2}{3}\left[\frac{f_\rho}{2M}\right]^2\hat{j}_a^{-2}\sum_b(2-\delta_{q_a,q_b})\frac{G_b(r)}{r^2}\sum_{\mathcal{J}L}\langle a||T_{\mathcal{J}L}||b\rangle[\langle a||T_{\mathcal{J}L}||b\rangle G_aG_b-\langle a'||T_{\mathcal{J}L}||b'\rangle F_aF_b]_r. \tag{B22}$$

The $VT$ contributions are

$$X^{(VT,1)}(r)=\left[\frac{g_\rho f_\rho}{2M}\right]m_\rho^2\hat{j}_a^{-2}\sum_b(2-\delta_{q_a,q_b})\sum_{LL_1}(-1)^{L_1}\hat{L}_1\begin{bmatrix}L_1 & L & 1\\ 0 & 0 & 0\end{bmatrix}$$
$$\times\left\{G_b(r)\langle a'||T_{LL_1}||b\rangle\int_0^\infty[\langle a||Y_L||b\rangle G_aG_b+\langle a'||Y_L||b'\rangle F_aF_b]_{r'}S_{LL_1}(r,r')dr'\right.$$
$$\left.+F_b(r)\langle a'||Y_L||b'\rangle\int_0^\infty[\langle a||T_{LL_1}||b'\rangle G_aF_b+\langle a'||T_{LL_1}||b\rangle F_aG_b]_{r'}S_{LL_1}(r',r)dr'\right\}, \tag{B23}$$

$$X^{(VT,2)}(r)=\sqrt{6}\left[\frac{g_\rho f_\rho}{2M}\right]m_\rho^2\hat{j}_a^{-2}\sum_b(2-\delta_{q_a,q_b})\sum_{fLL_1}(-1)^f f_{Lf}(L_1)$$
$$\times\left\{F_b(r)\langle a'||T_{fL_1}||b'\rangle\int_0^\infty[\langle a||T_{fL}||b'\rangle G_aF_b-\langle a'||T_{fL}||b\rangle F_aG_b]_{r'}S_{LL_1}(r,r')dr'\right.$$
$$\left.+G_b(r)\langle a'||T_{fL}||b\rangle\int_0^\infty[\langle a||T_{fL_1}||b\rangle G_aG_b-\langle a'||T_{fL_1}||b'\rangle F_aF_b]_{r'}S_{LL_1}(r',r)dr'\right\}, \tag{B24}$$

where

$$S_{LL_1}(r,r')=\tilde{I}_{L_1}(z)\tilde{K}_L(z')\theta(z'-z)-\tilde{I}_L(z')\tilde{K}_{L_1}(z)\theta(z-z') . \tag{B25}$$

The expression for $Y^{(VT,1)}$ can be obtained from $X^{(VT,1)}$ by replacing $G_b(r)\langle a'||T_{LL_1}||b\rangle$ and $F_b(r)\langle a'||Y_L||b'\rangle$ by $F_b(r)\langle a||T_{LL_1}||b'\rangle$ and $G_b(r)\langle a||Y_L||b\rangle$, respectively. In $X^{(VT,2)}$ the replacement of $F_b(r)\langle a'||T_{fL_1}||b'\rangle$ and $G_b(r)\langle a'||T_{fL}||b\rangle$ by $G_b(r)\langle a||T_{fL_1}||b\rangle$ and $F_b(r)\langle a||T_{fL}||b'\rangle$, respectively, and an overall change of sign leads to $Y^{(VT,2)}$.

## APPENDIX C: NUMERICAL SOLUTION OF THE HARTREE-FOCK EQUATIONS

The HF equations (60) are a set of coupled integro-differential equations that has to be solved self-consistently. The major complication is due to the Fock contributions which give rise to the integral terms, i.e., the HF potentials are fully nonlocal and state dependent. It is advantageous, in practice, to rewrite the HF equations in a completely equivalent form of a set of homogeneous differential equations. One possible way of achieving this goal is to write the inhomogeneous terms as

$$X_a(r)=\frac{G_a(r)X_a(r)}{G_a^2(r)+F_a^2(r)}G_a(r)+\frac{F_a(r)X_a(r)}{G_a^2(r)+F_a^2(r)}F_a(r)$$
$$\equiv P_a(r)G_a(r)+Q_a(r)F_a(r) , \tag{C1}$$

$$Y_a(r)\equiv R_a(r)G_a(r)+S_a(r)F_a(r) , \tag{C2}$$

the definition of $R_a(r)$ and $S_a(r)$ being similar to that of $P_a(r)$ and $Q_a(r)$. The HF equations (60) then become

$$\frac{d}{dr}\begin{bmatrix}G_a(r)\\F_a(r)\end{bmatrix}=\begin{bmatrix}-\frac{\kappa_a}{r}-\Sigma_{T,a}^D(r)-P_a(r) & M+E_a+\Sigma_{S,a}^D(r)-\Sigma_{0,a}^D(r)-Q_a(r)\\ M-E_a+\Sigma_{S,a}^D(r)+\Sigma_{0,a}^D(r)+R_a(r) & \frac{\kappa_a}{r}+\Sigma_{T,a}^D(r)+S_a(r)\end{bmatrix}\begin{bmatrix}G_a(r)\\F_a(r)\end{bmatrix} . \tag{C3}$$

The structure of the equations is the same as that encountered in the simple Hartree approximation, except that the potentials are now more complicated. In the current literature one usually transforms the coupled first-order equations into a second-order differential equation for the upper component $G_a(r)$. We have preferred instead to solve Eqs. (C3) directly by a standard fourth-order Runge-Kutta method. Convergence toward the self-consistent solution requires generally 20 iterations or less. Our convergence criterion is that all the $E_a$'s should change by less than 50 keV over several iterations.

The integrals involved in the expressions of the potentials are evaluated using Simpson's rule. The stability of the numerical results has been checked by changing the length of the integration step. We find that a step of 0.10 fm is sufficient for the desired accuracy.

[1]H. A. Bethe, Annu. Rev. Nucl. Sci. **21**, 93 (1971).
[2]D. Vautherin and D. M. Brink, Phys. Rev. C **5**, 626 (1972).
[3]L. D. Miller and A. E. S. Green, Phys. Rev. C **5**, 241 (1972); L. D. Miller, *ibid.* **9**, 537 (1974).
[4]J. D. Walecka, Ann. Phys. (N.Y.) **83**, 491 (1974).
[5]S. A. Chin, Ann. Phys. (N.Y.) **108**, 1301 (1977).
[6]R. Brockmann, Phys. Rev. C **18**, 1510 (1978).
[7]L. N. Savushkin, Yad. Fiz. **30**, 660 (1979) [Sov. J. Nucl. Phys. **30**, 340 (1979)].
[8]C. J. Horowitz and B. D. Serot, Nucl. Phys. **A368**, 503 (1981).
[9]J. Boguta, Nucl. Phys. **A371**, 386 (1982).
[10]M. Jaminon, C. Mahaux, and P. Rochus, Phys. Rev. C **22**,

2027 (1980); Nucl. Phys. **A365**, 371 (1981).
[11]C. J. Horowitz and B. D. Serot, Nucl. Phys. **A399**, 529 (1983).
[12]M. R. Anastasio, L. S. Celenza, W. S. Pong, and C. M. Shakin, Phys. Rep. **100**, 327 (1983).
[13]R. Brockmann and R. Machleidt, Phys. Lett. **149B**, 283 (1984).
[14]R. Brockmann and W. Weise, Nucl. Phys. **A355**, 365 (1981).
[15]J. Boguta, Phys. Lett. **106B**, 250 (1981); J. Boguta and H. Stöcker, *ibid.* **120B**, 289 (1983).
[16]A. Bouyssy, S. Marcos, and Pham Van Thieu, Nucl. Phys. **A422**, 541 (1984).
[17]B. D. Serot and J. D. Walecka, in *Advances in Nuclear Physics*, edited by J. W. Negele and E. Vogt (Plenum, New York, 1986), Vol. 16.
[18]J. Sucher, Phys. Rev. A **22**, 348 (1980); M. H. Mittleman, *ibid.* **24**, 1167 (1981).
[19]J. D. Bjorken and S. D. Drell, *Relativistic Quantum Mechanics* (McGraw-Hill, New York, 1964).
[20]A. Bouyssy, Nucl. Phys. **A381**, 445 (1982).
[21]A. Bouyssy, S. Marcos, J.-F. Mathiot, and Nguyen Van Giai, Phys. Rev. Lett. **55**, 1731 (1985).
[22]M. Jaminon, Nucl. Phys. **A402**, 366 (1983).
[23]M. Bawin and M. Jaminon, Nucl. Phys. **A407**, 515 (1983).
[24]G. E. Brown, W. Weise, G. Boym, and J. Speth, Comments Nucl. Part. Phys. **17**, 39 (1987).
[25]X. Campi and D. W. L. Sprung, Nucl. Phys. **A194**, 401 (1972).
[26]C. Mahaux, P. F. Bortignon, R. A. Broglia, and C. H. Dasso, Phys. Rep. **120**, 1 (1985).
[27]B. Frois, in Proceedings of the International Conference on Nuclear Physics, Florence, Italy, 1983, p. 221.
[28]A. Bouyssy, S. Marcos, and J.-F. Mathiot, Nucl. Phys. **A415**, 497 (1984).
[29]W. Bentz, A. Arima, H. Hyuga, K. Shimizu, and K. Yazaki, Nucl. Phys. **A436**, 593 (1985).
[30]H. Kurazawa and T. Suzuki, Phys. Lett. **165B**, 234 (1985).
[31]R. L. Birbrair, L. N. Savushkin, and V. N. Fomenko, Yad. Fiz. **35**, 1134 (1982) [Sov. J. Nucl. Phys. **35**, 664 (1982)].
[32]J. Boguta and S. A. Moszkowski, Nucl. Phys. **A403**, 445 (1983).
[33]A. Bouyssy and S. Marcos, Phys. Lett. **127B**, 157 (1983).
[34]M. Beiner, H. Flocard, Nguyen Van Giai, and P. Quentin, Nucl. Phys. **A238**, 29 (1975).
[35]L. D. Miller, Phys. Rev. Lett. **28**, 1281 (1972).
[36]A. D. Jackson, Annu. Rev. Nucl. Part. Sci. **33**, 105 (1983).